SURFCLAM FIGURES

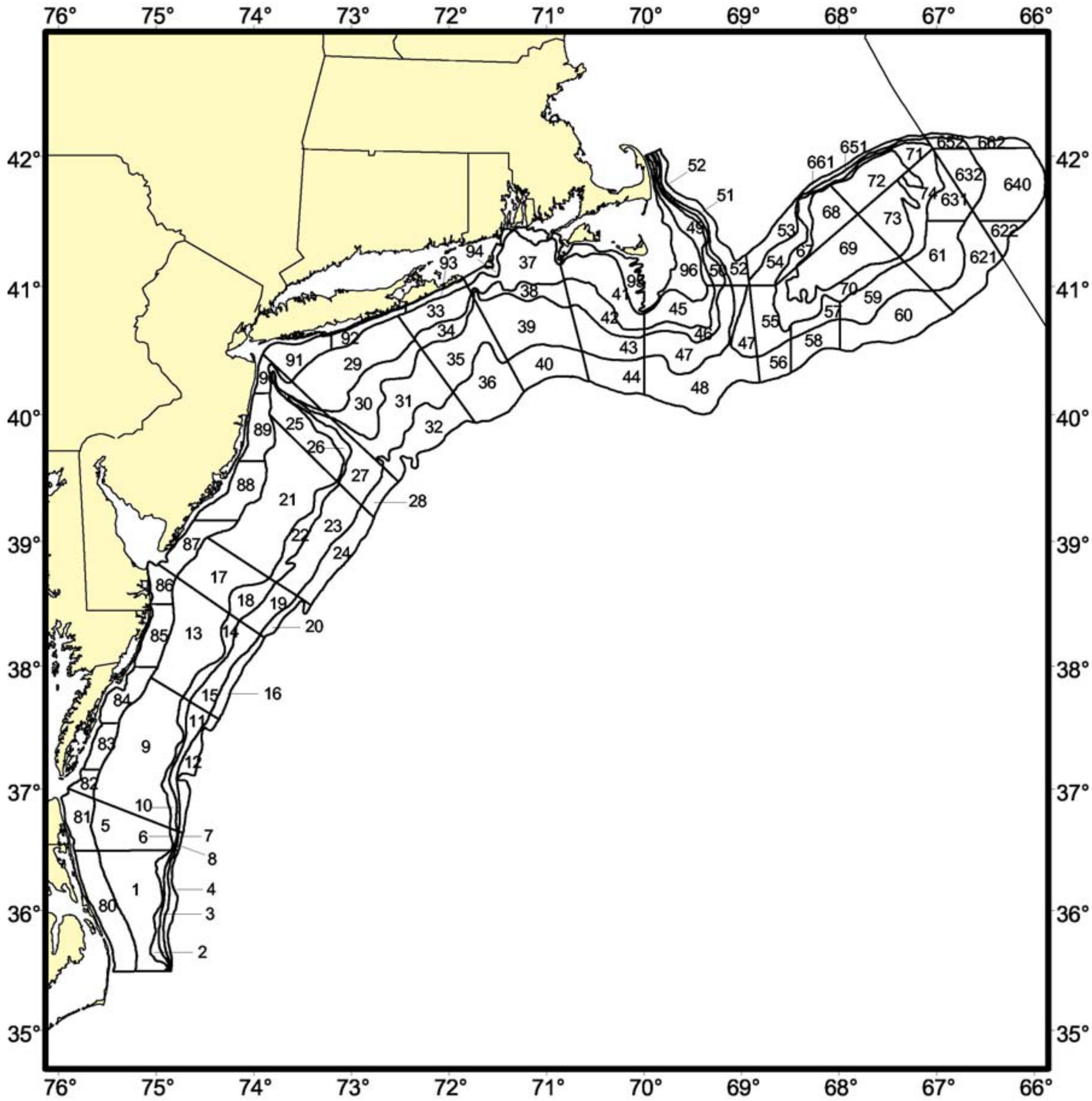

Figure C1. Surfclam stock assessment regions and NEFSC clam survey strata. Northern and southern New Jersey is combined to form the larger New Jersey (NJ) assessment region.

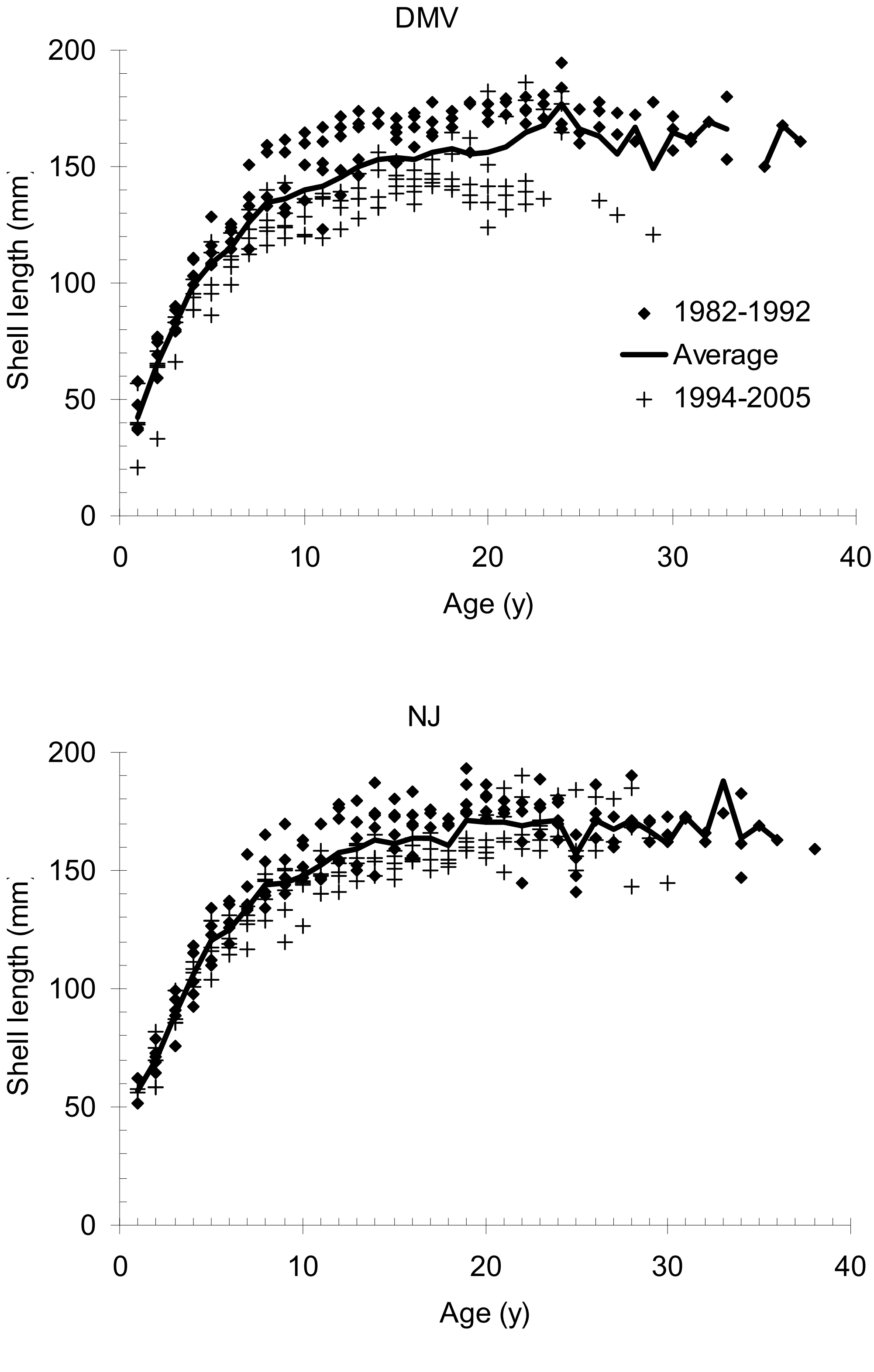

Figure C2. Size at age data for surfclam in DMV and NJ from NEFSC clam surveys during 1982-1992 and 1994-2005. The dark line shows average size at age in all years.

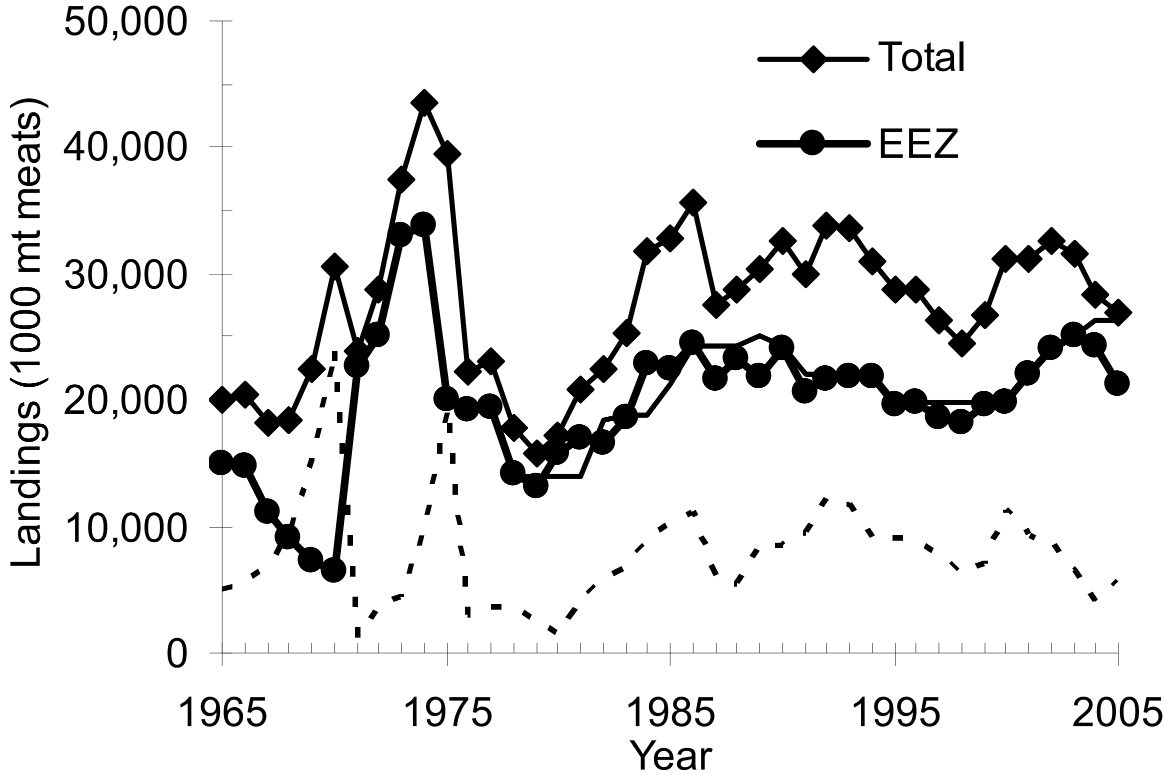

Figure C3. Atlantic surfclam landings and EEZ surfclam quotas (all converted to mt meats).

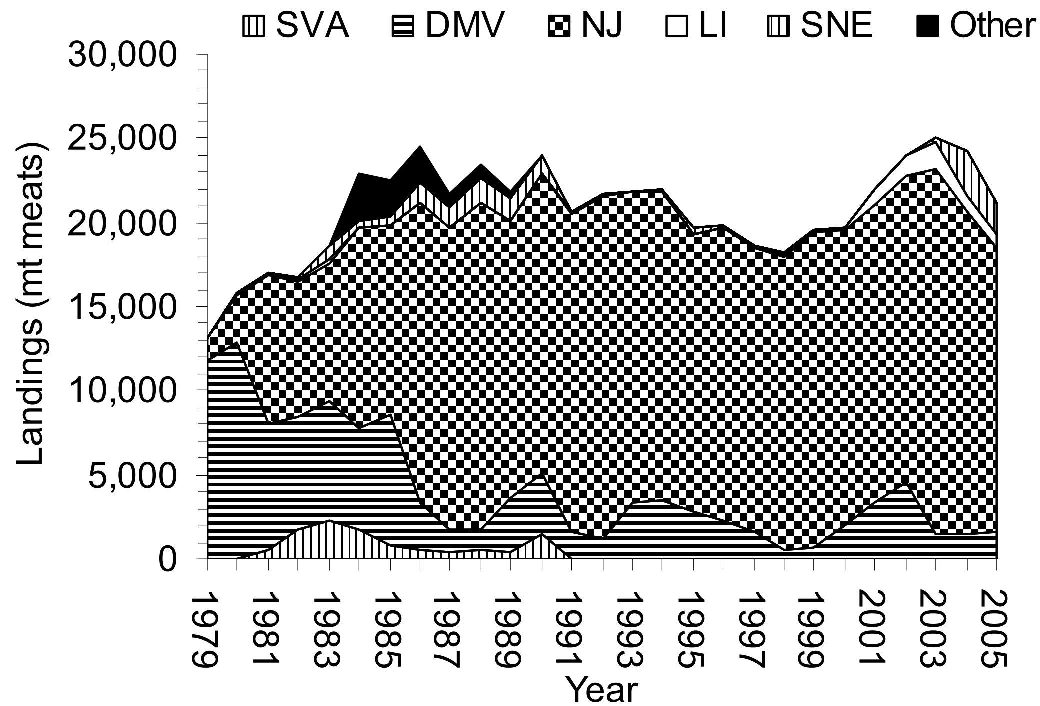

Figure C4. Surfclam landings from the US EEZ during 1979-2005 by stock assessment region.

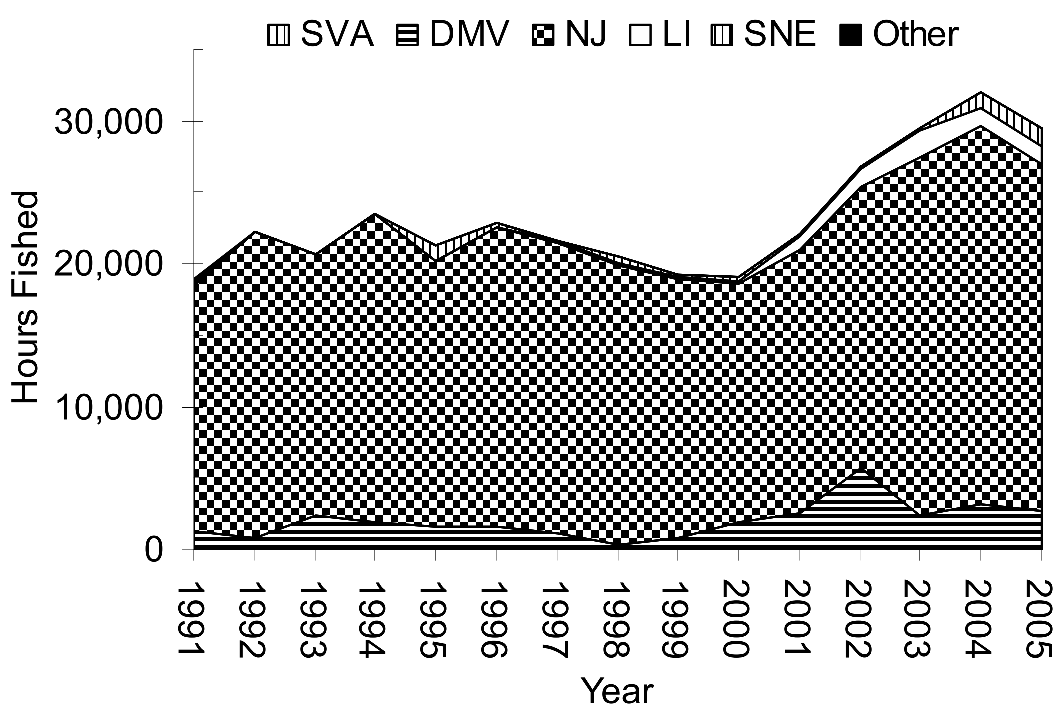

Figure C5. Total fishing effort (hours fished, all trips and all vessels) in the US EEZ during 1991-2005 by stock assessment region.

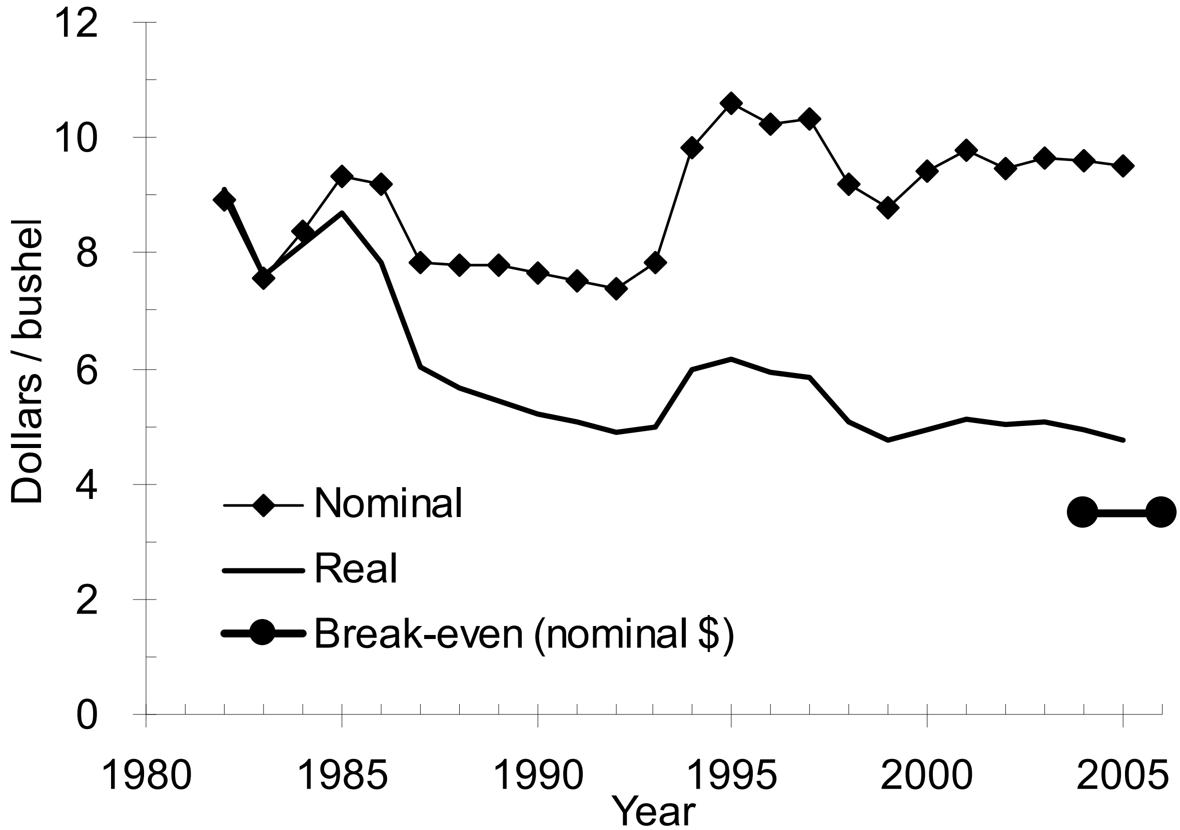

Figure C6. Real and nominal exvessel prices (US$ per bushel) for surfclam landed (EEZ and state waters) during 1982-2005. Real prices use 1980-1982 as the base year. The current "break-even" price (to meet variable costs) is about 3-4 $ bu-1 (nominal, in 2005 dollars) and shown for comparison.

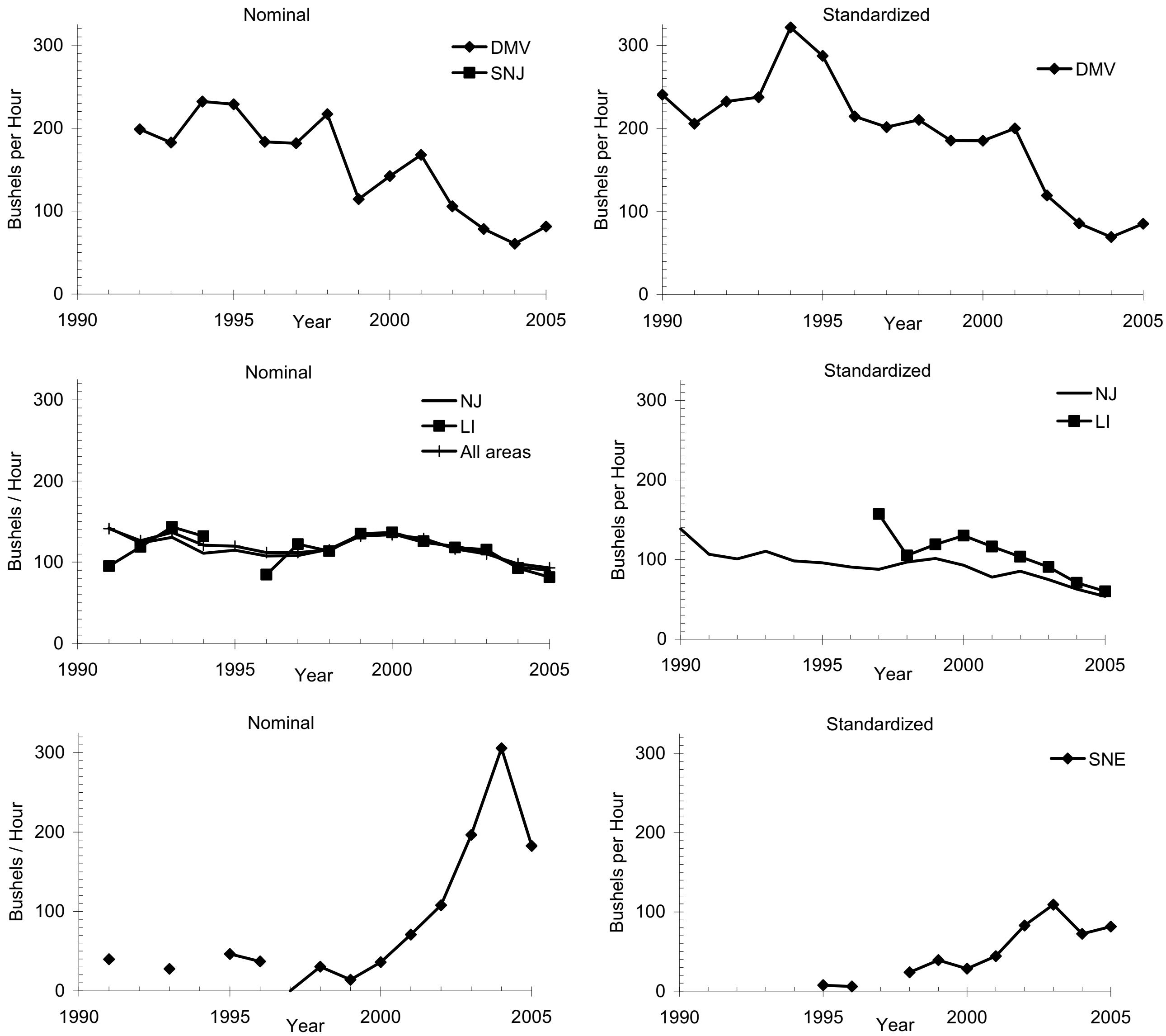

Figure C7. Nominal and standardized LPUE for surfclam in the EEZ, by region. Regions with similar trends are plotted together.

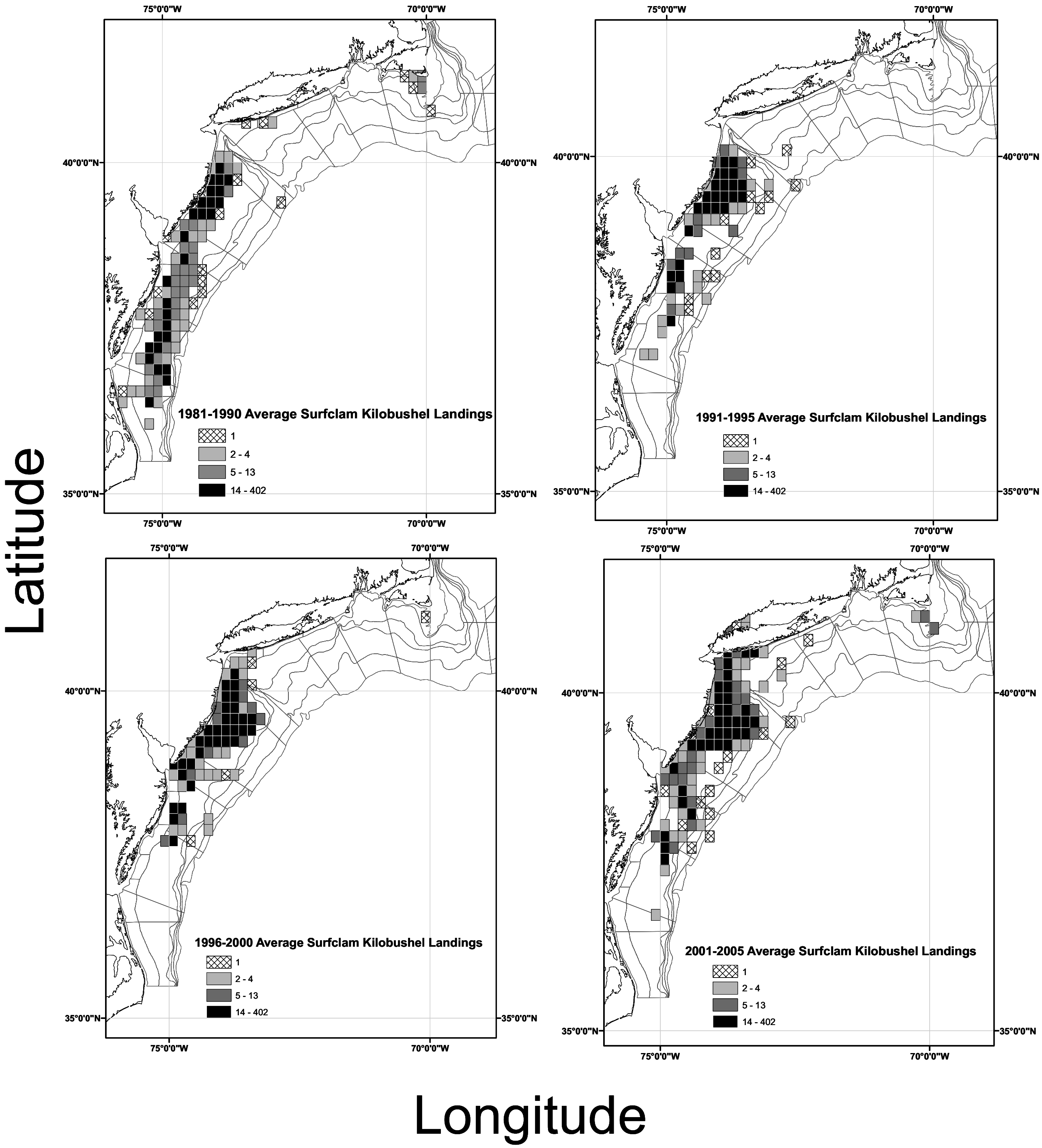

Figure C8. Spatial distribution of surfclam landings (annual means, 1 kilobushel = 1000 bu y-1) during 1981-1990, 1991-1995, 1996-2000 and 2001-2005 based on logbook data and ten-minute squares. Categories correspond approximately with quartiles during 1981-1990.

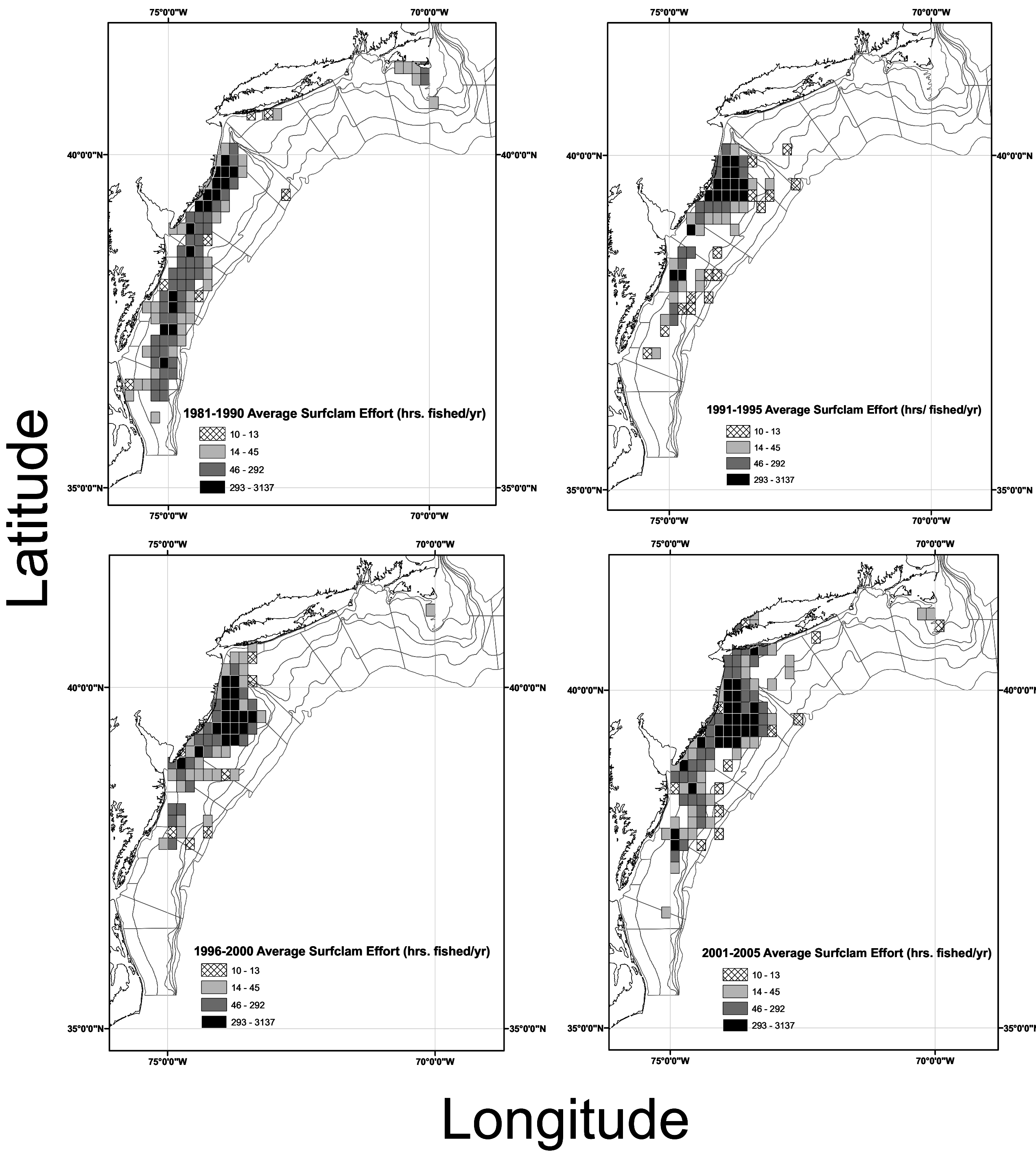

Figure C9. Spatial distribution of surfclam fishing effort (annual means, h y^{-1}) during 1981-1990, 1991-1995, 1996-2000 and 2001-2005 based on logbook data and ten-minute squares. Categories correspond approximately with quartiles during 1981-1990.

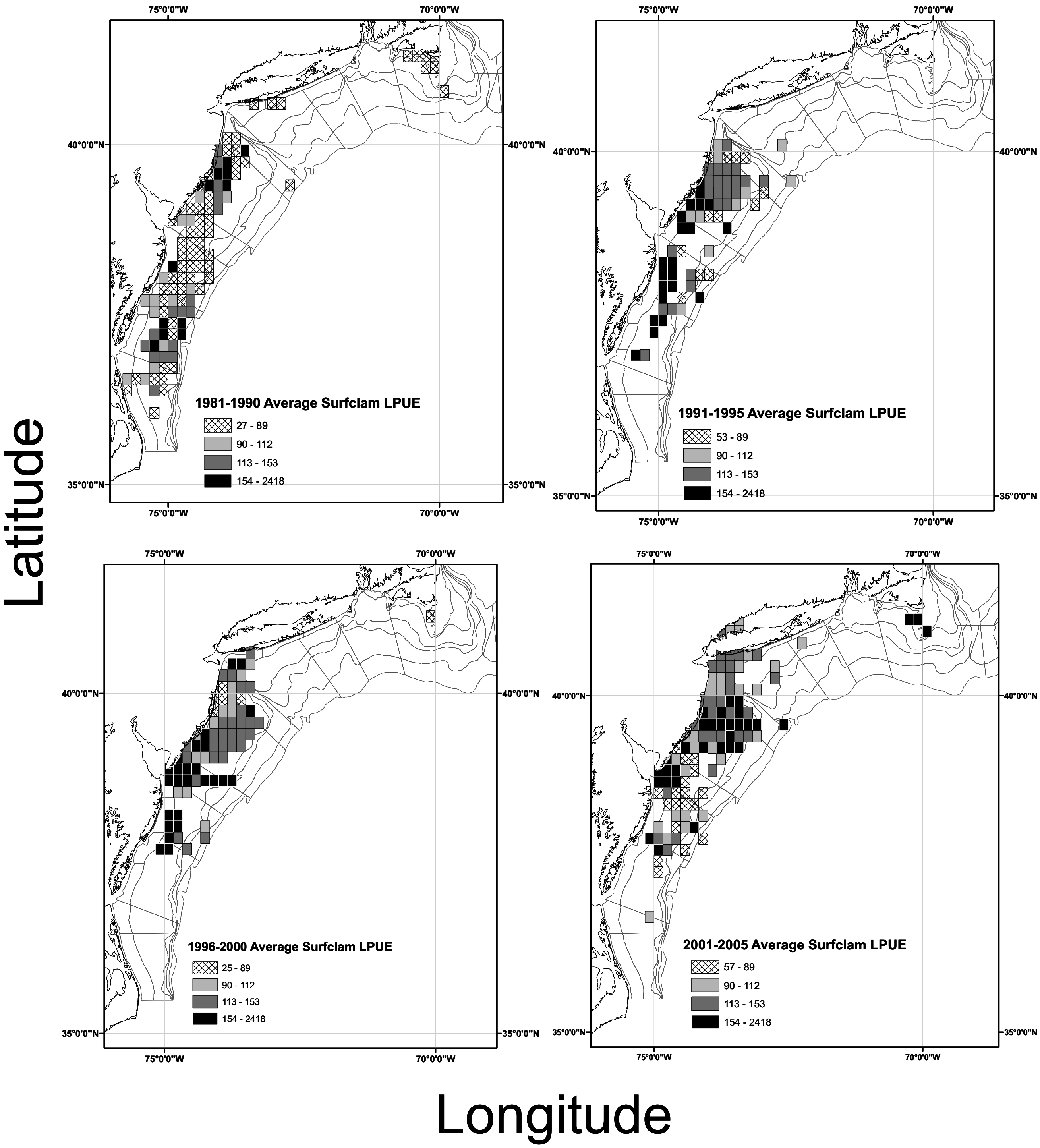

Figure C10. Spatial distribution of surfclam LPUE (annual means, bu h^{-1} y^{-1}) during 1981-1990, 1991-1995, 1996-2000 and 2001-2005 based on logbook data and ten-minute squares. Categories correspond approximately with quartiles during 1981-1990.

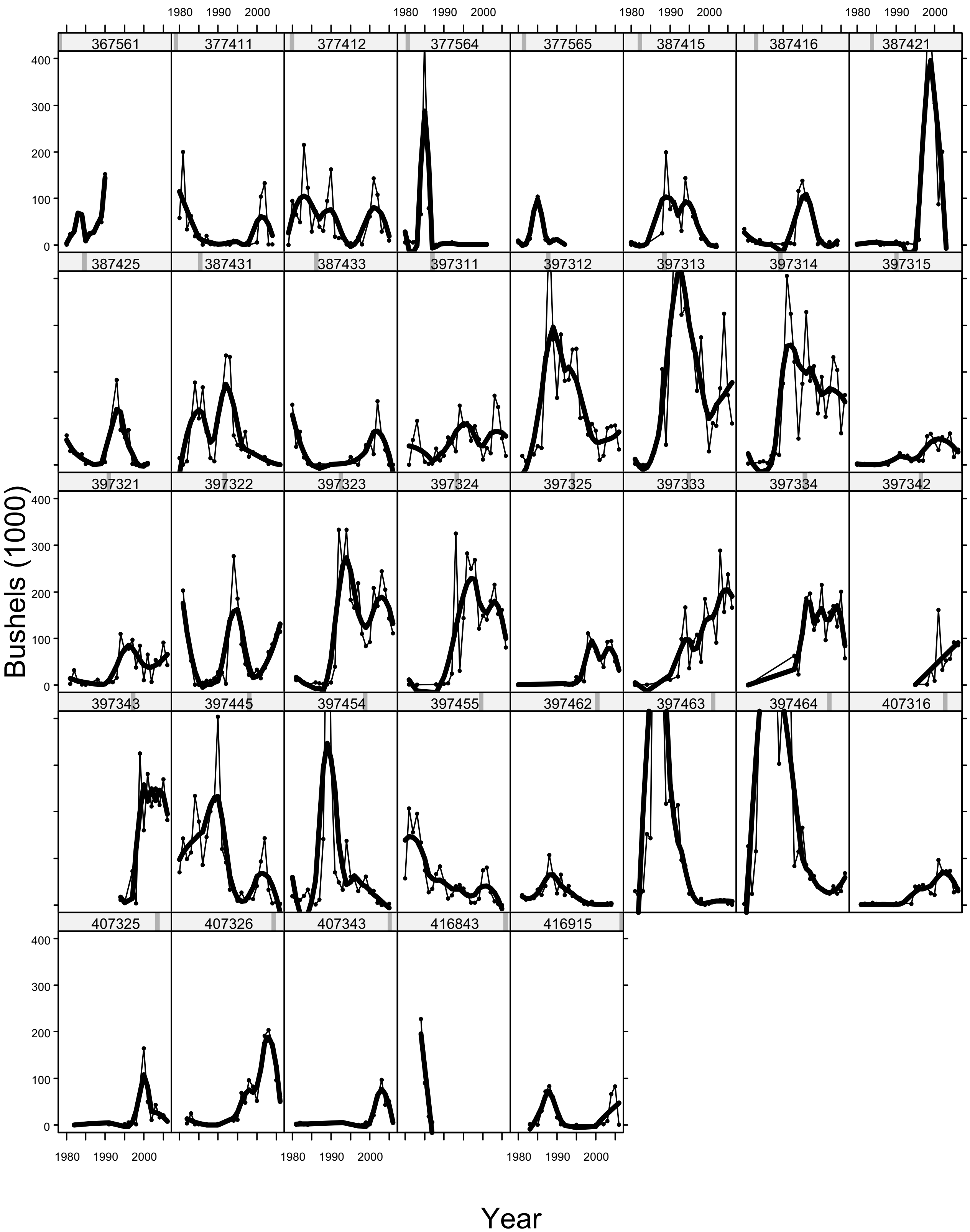

Figure C11. Annual surfclam landings (1000 bushels per year) for important ten-minute squares during 1980-2005 based on logbook data. The smooth dark line is a spline intended to show general trends.

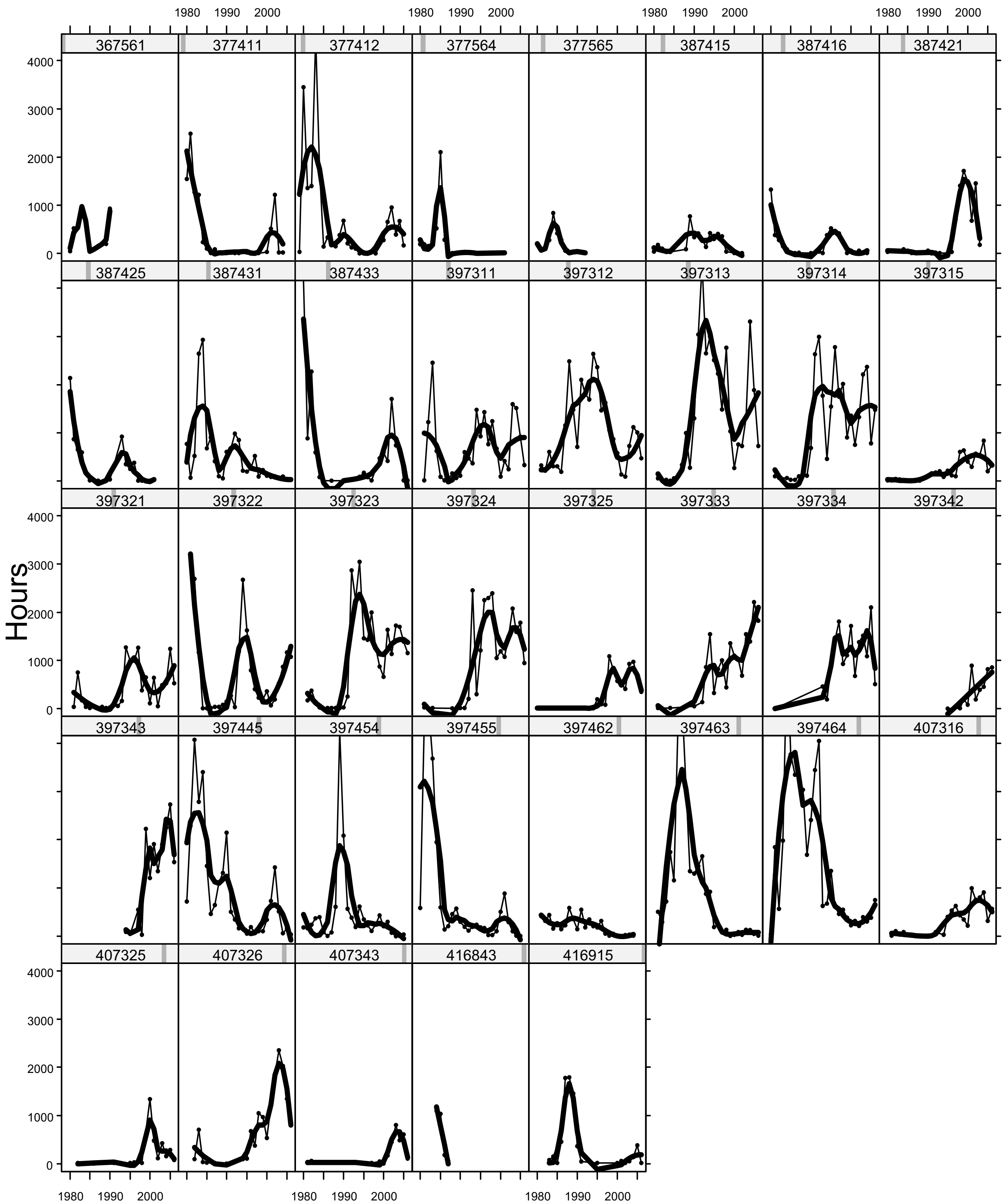

Figure C12. Annual surfclam fishing effort (hours of fishing per year) for important ten-minute squares during 1980-2005 based on logbook data. The smooth dark line is a spline intended to show general trends.

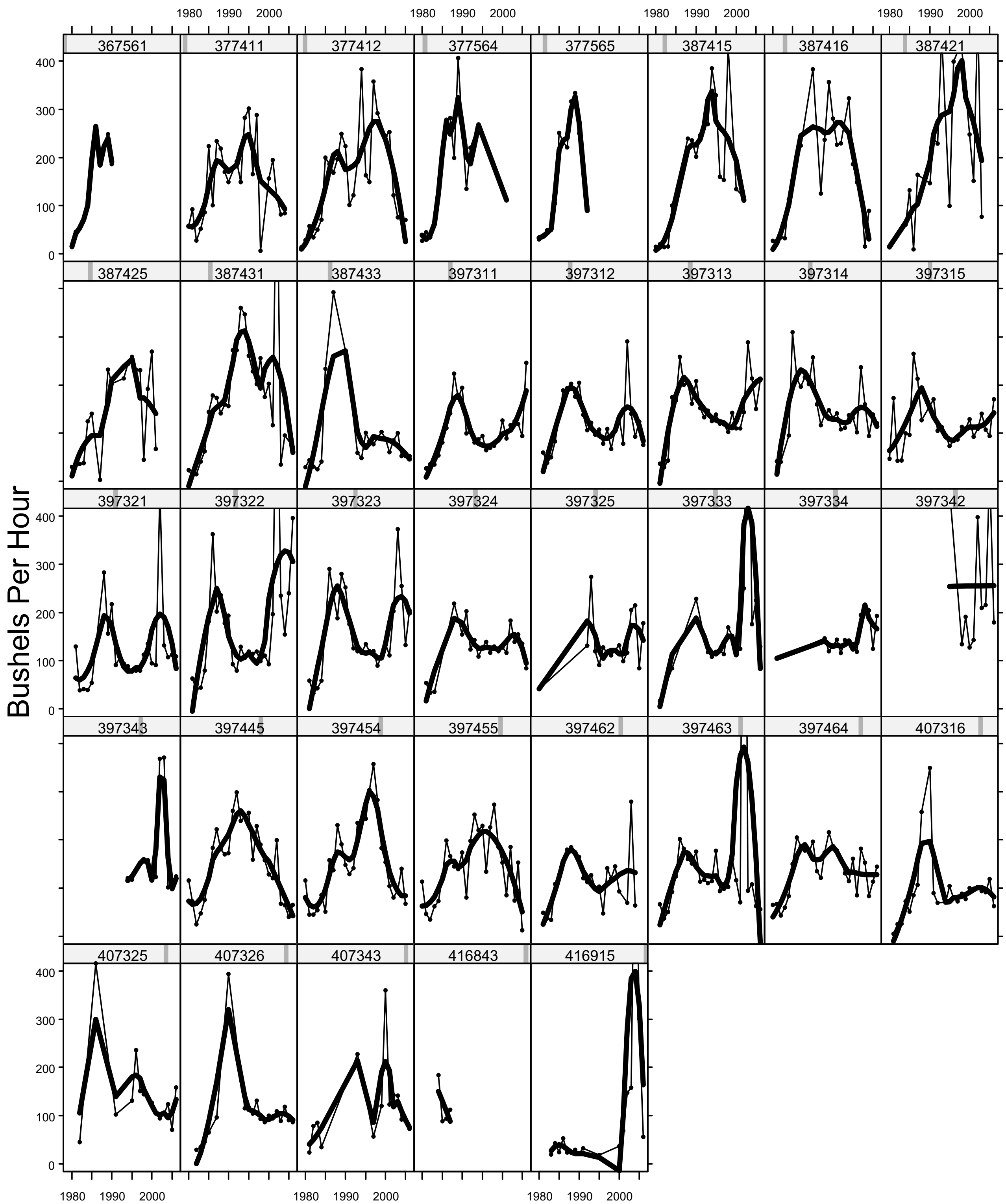

Figure C13. Annual surfclam landings per unit of fishing effort (LPUE, mean h^{-1}) for important ten-minute squares during 1980-2005 based on logbook data. The smooth dark line is a spline intended to show general trends.

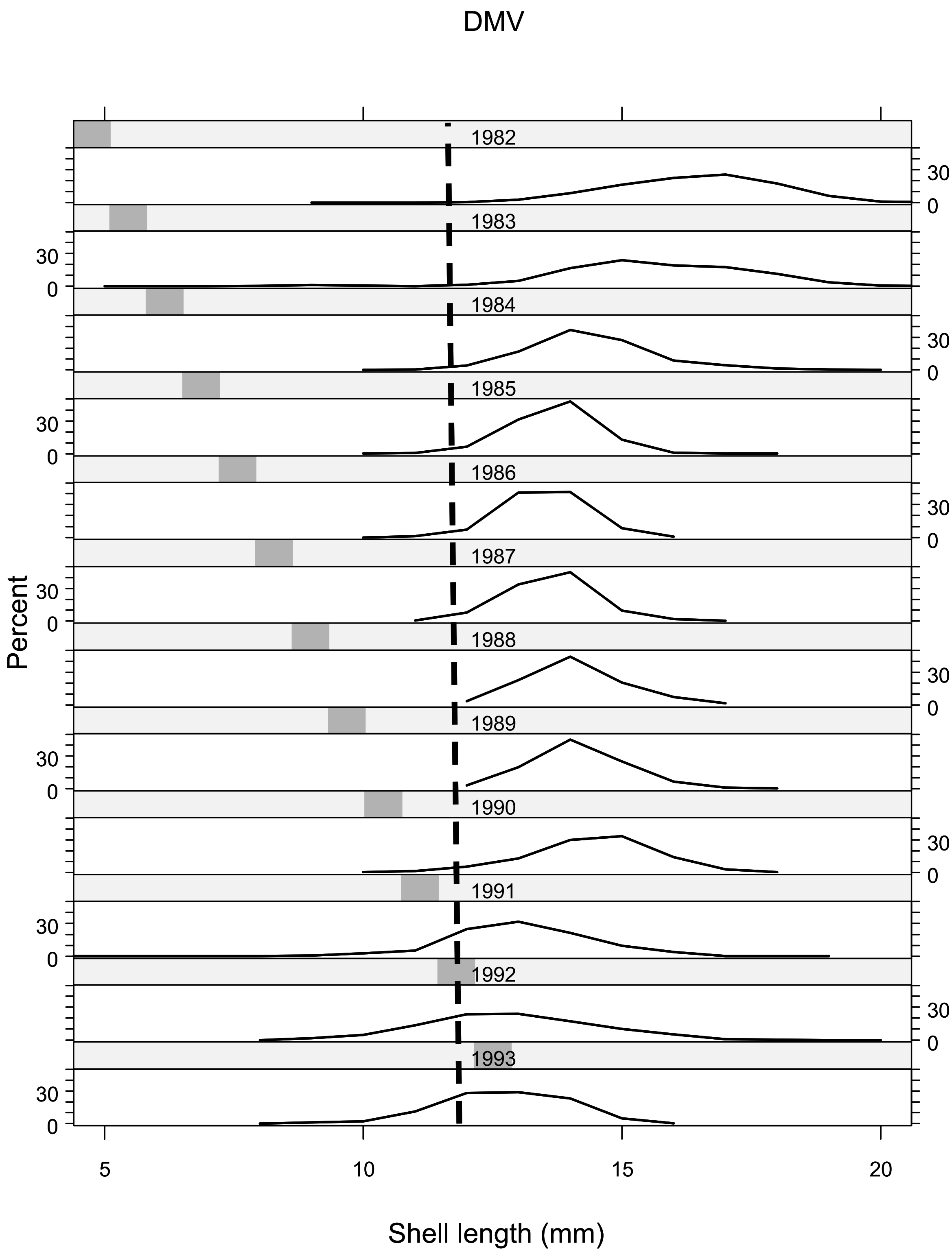

Figure C14. Commercial length composition data for surfclam caught in the DMV area, based on port samples. The dashed vertical line is at 120 mm SL.

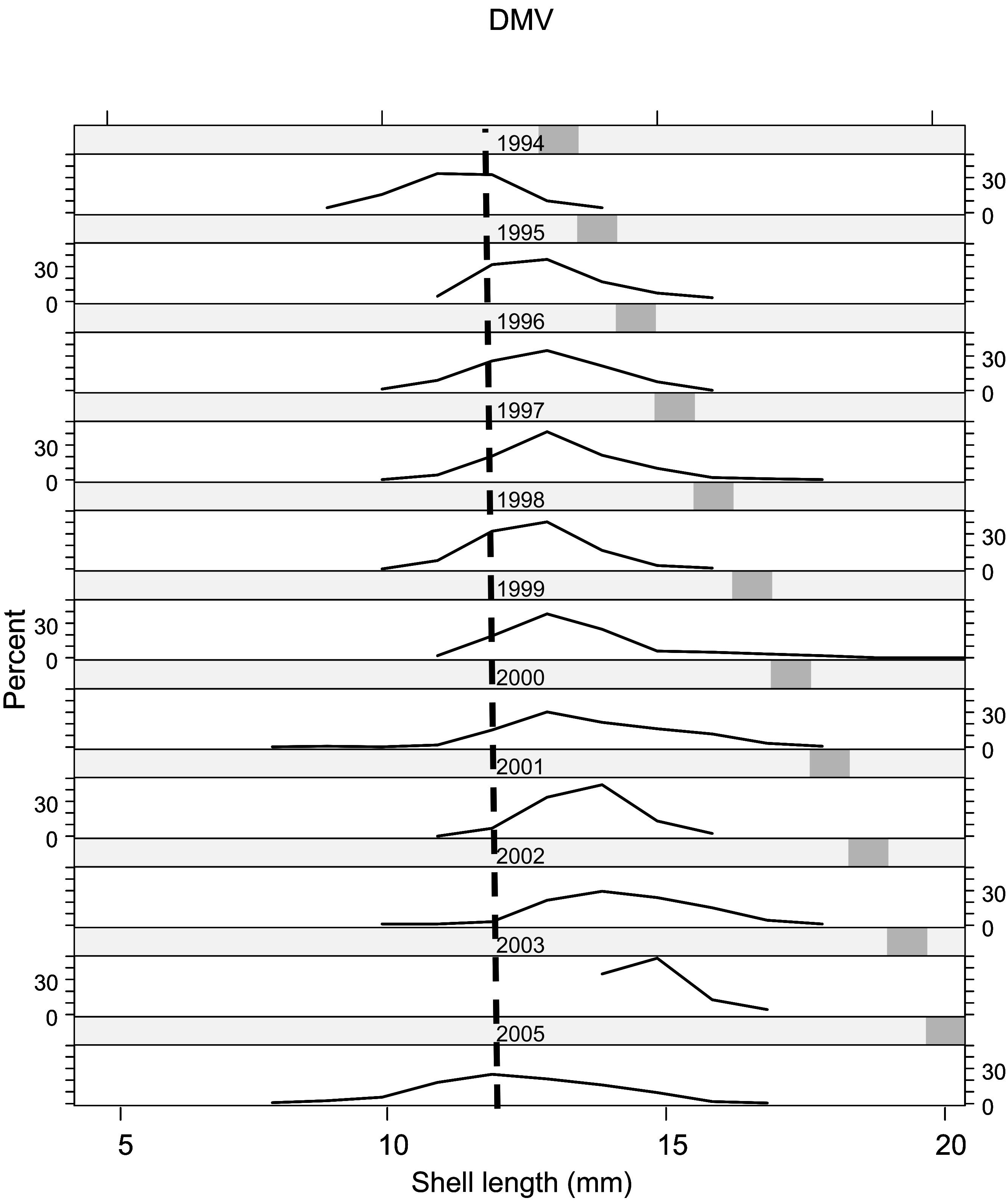

Figure C14. (continued)

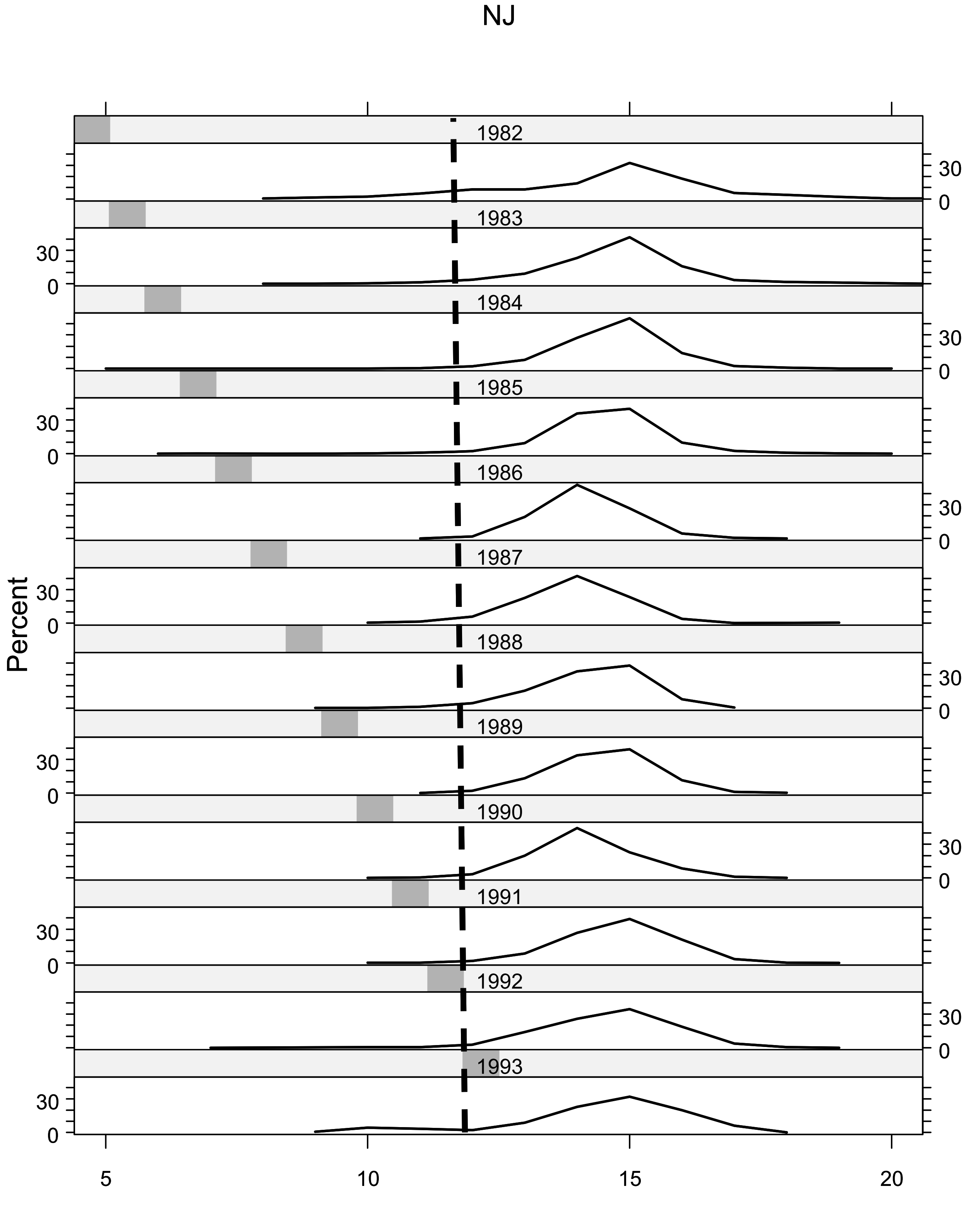

Figure C14. (continued)

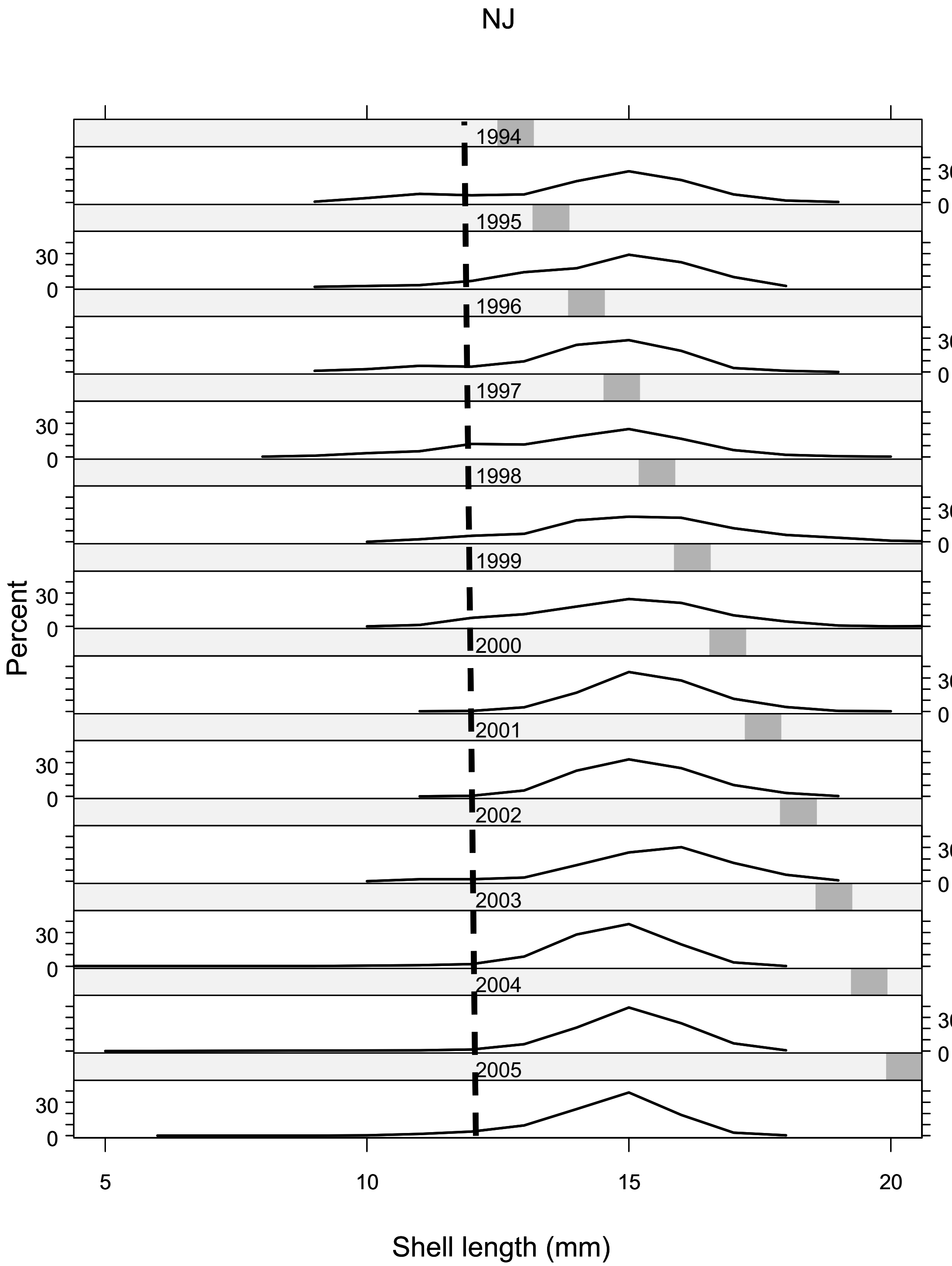

Figure C15. Commercial length composition data for surfclam caught in the NJ area, based on port samples. The dashed vertical line is at 120 mm SL.

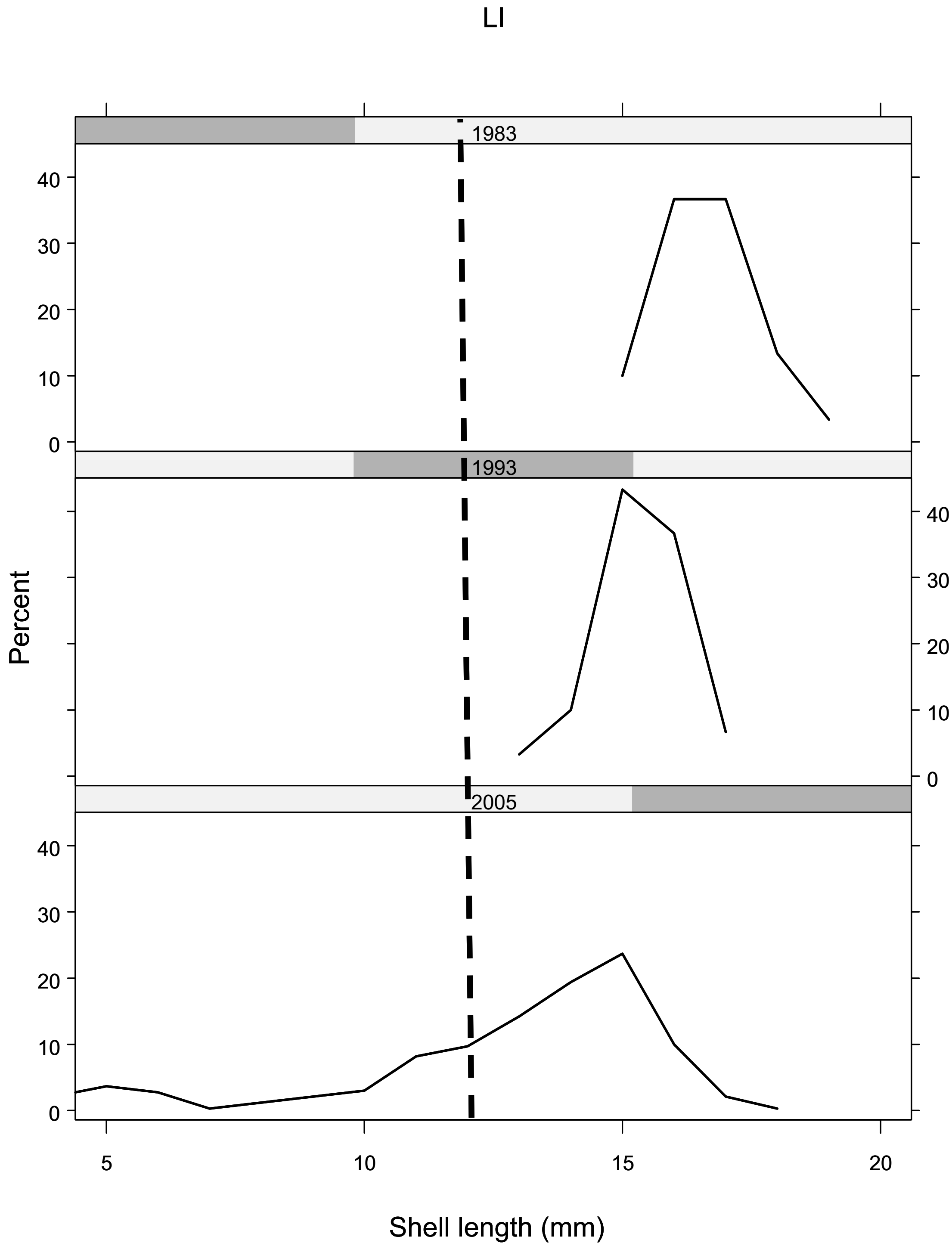

Figure C16. Commercial length composition data for surfclam caught in the LI area, based on port samples. The dashed vertical line is at 120 mm SL.

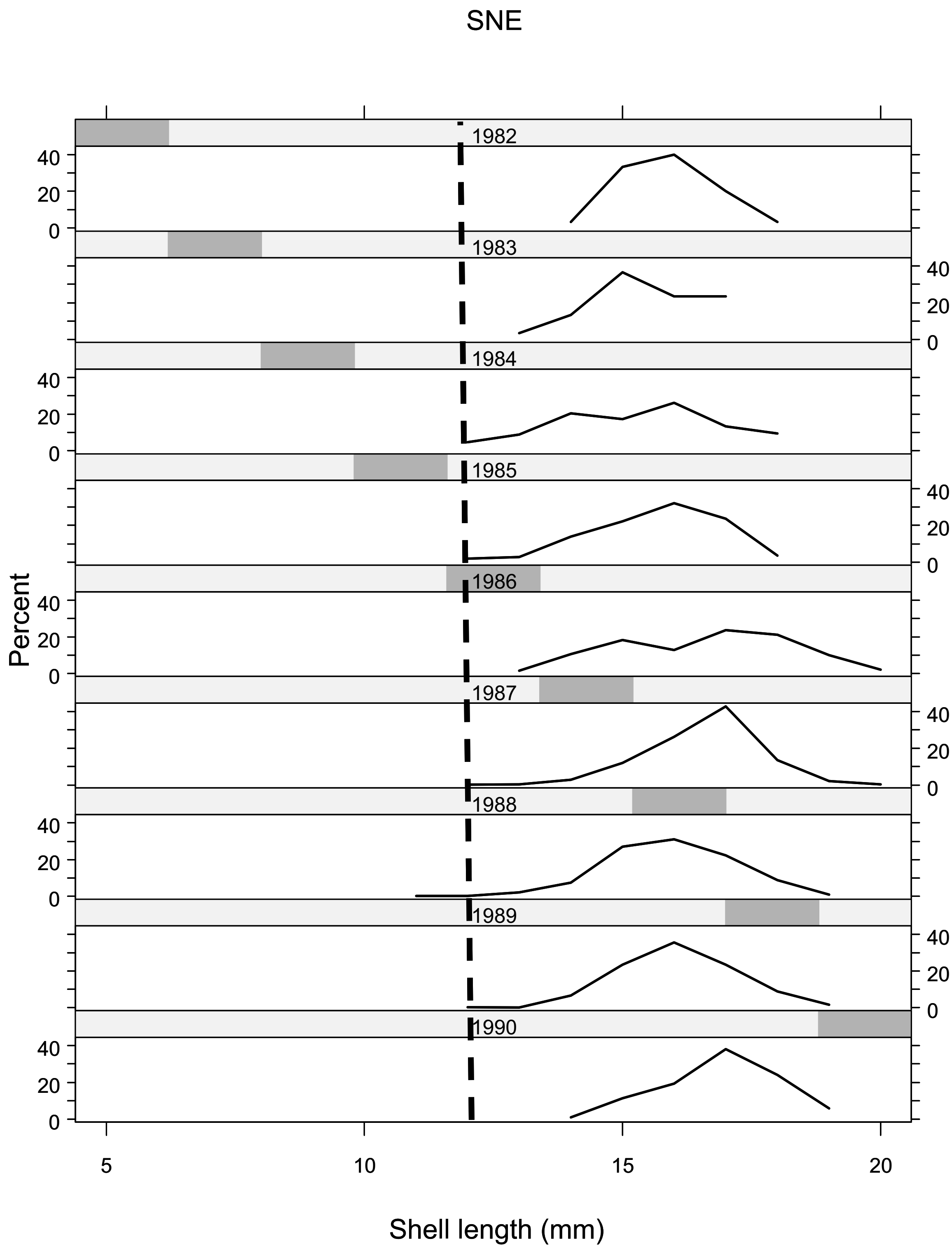

Figure C17. Commercial length composition data for surfclam caught in the SNE area, based on port samples. The dashed vertical line is at 120 mm SL.

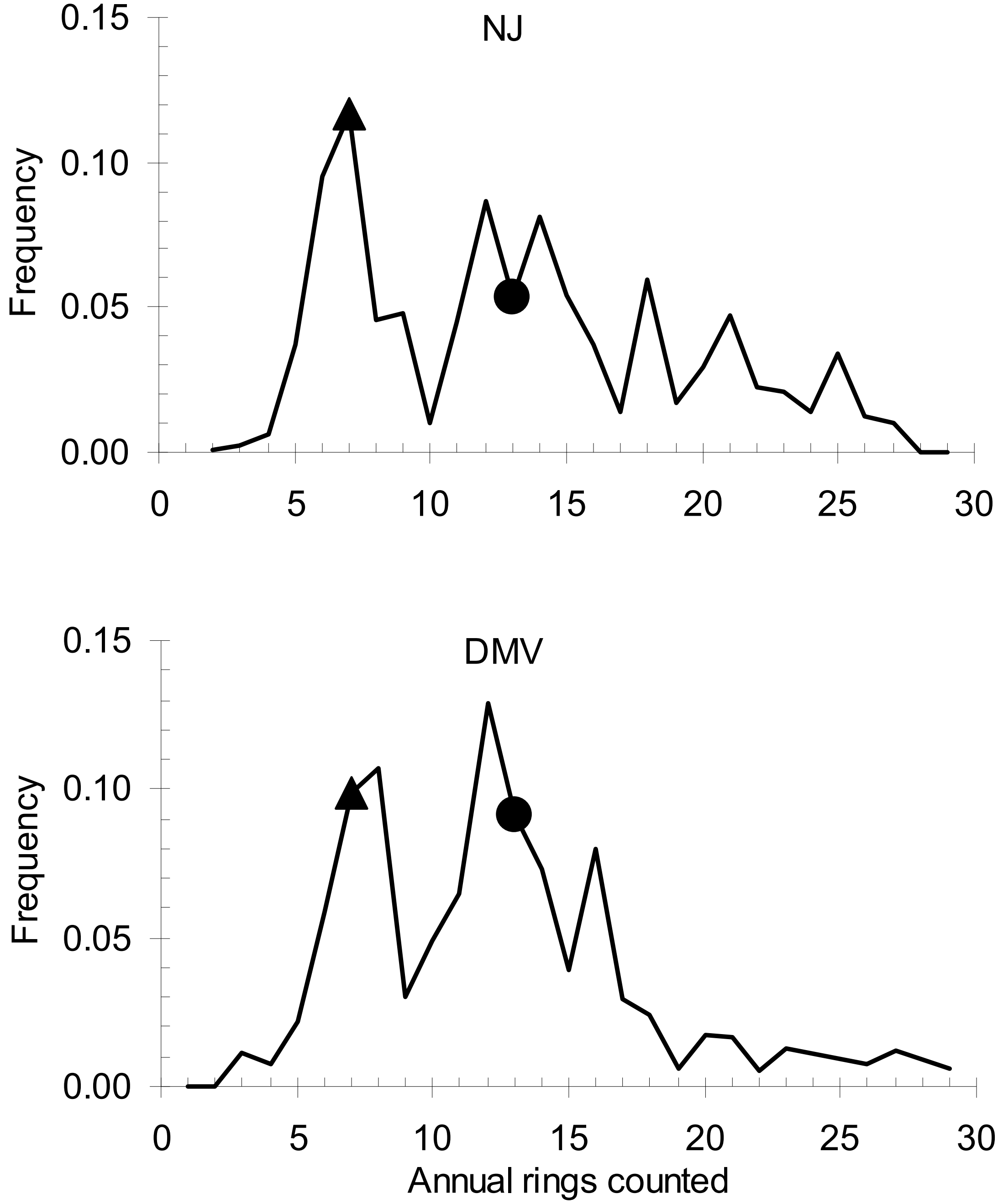

Figure C18. Commercial age composition data for surfclam in the NJ and DMV areas during 2005. There is uncertainty about timing of ring formation. Assuming rings form during the fall after the NEFSC clam survey, dark circles identify the 1992 (14 rings in 2005) year class and dark triangles identify the 1999 year class (7 rings in 2005).

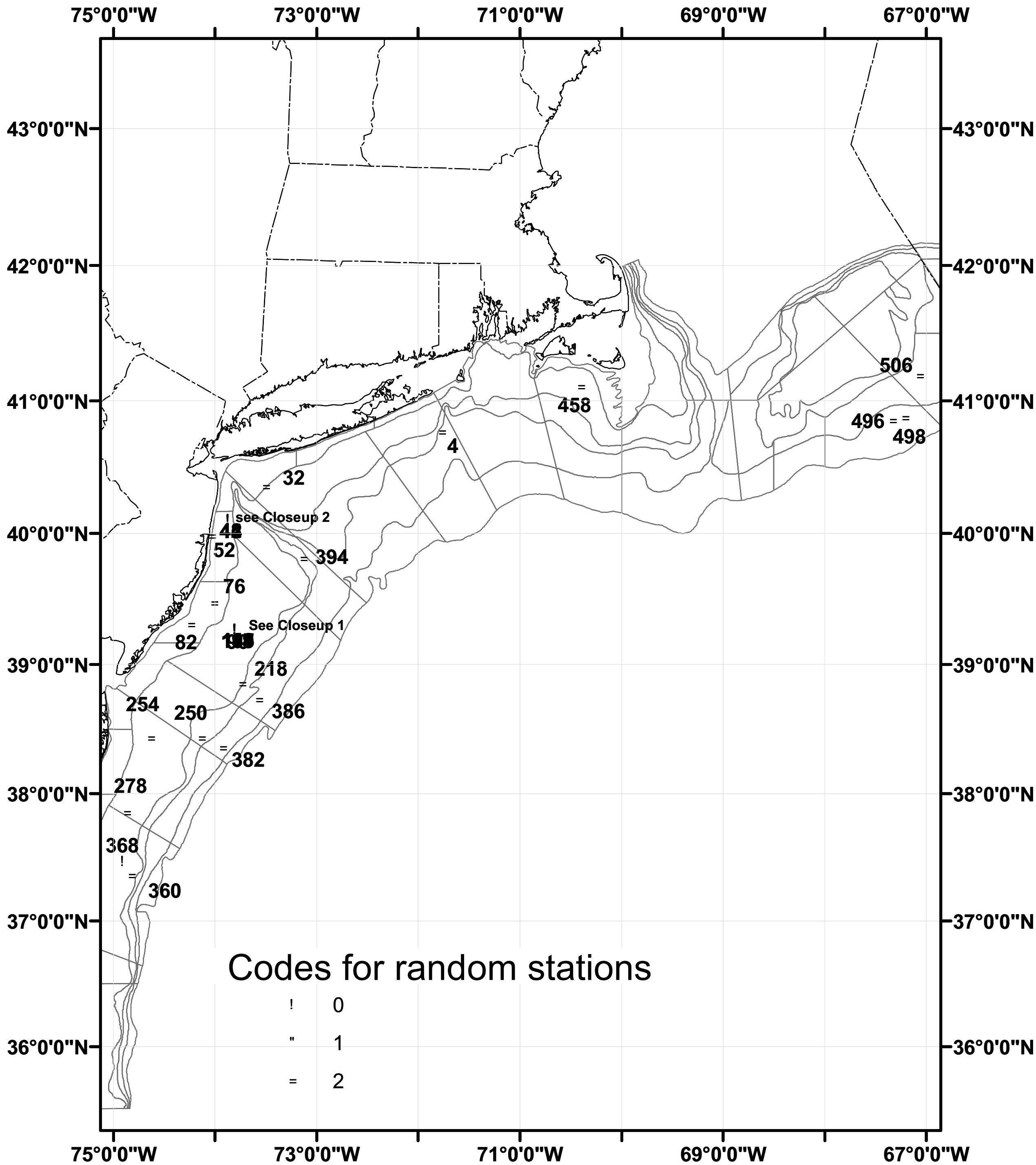

Figure C19. Locations of 2002 survey stations with poor dredge performance that would not have been excluded from trend and swept area trend analyses based on haul or gear damage codes, with station numbers. Codes 1 and 2 (dark squares and open circles) are random stations. Stations in close-up 1 are all from a depletion experiment.

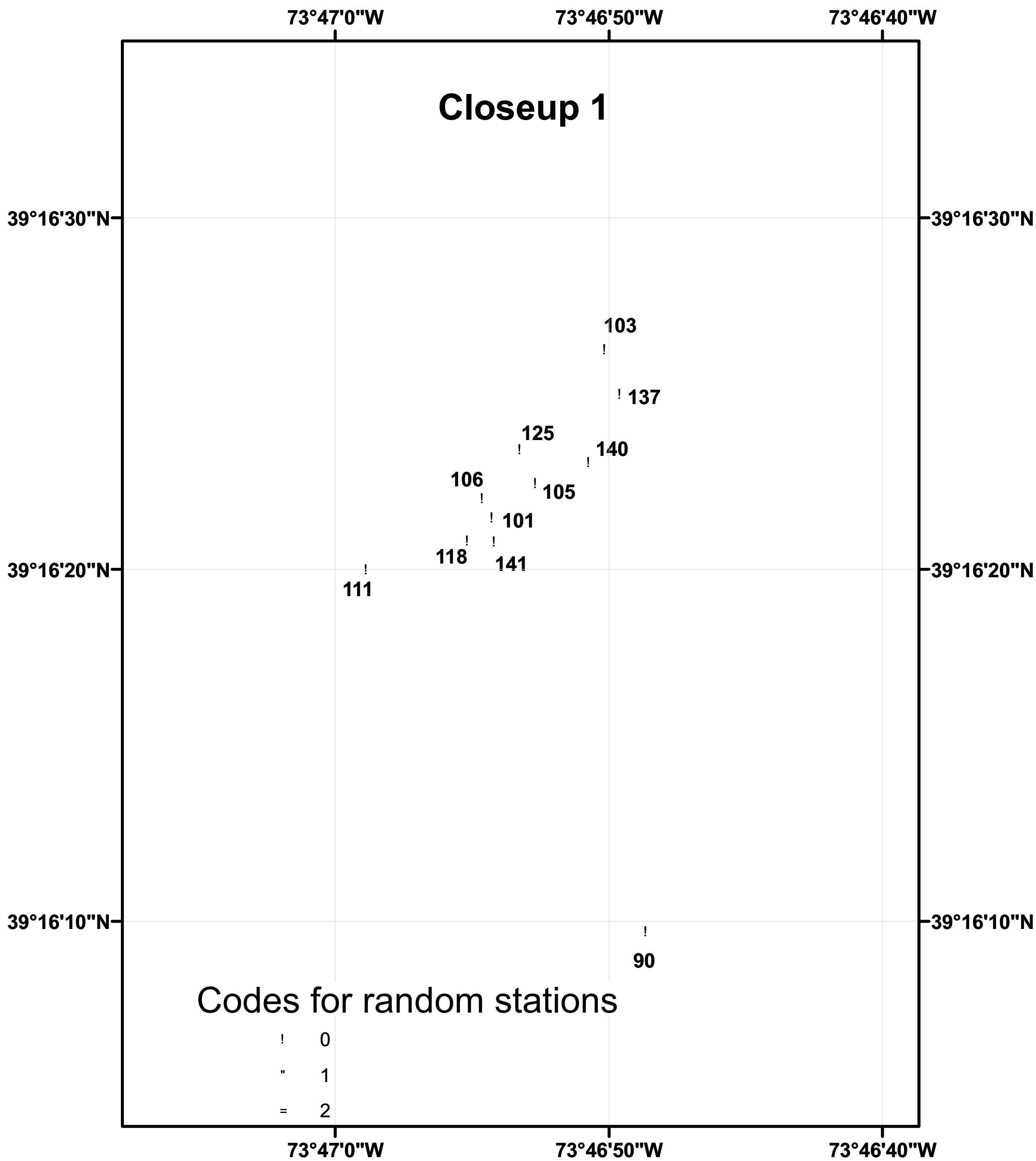

Figure C19 (continued)

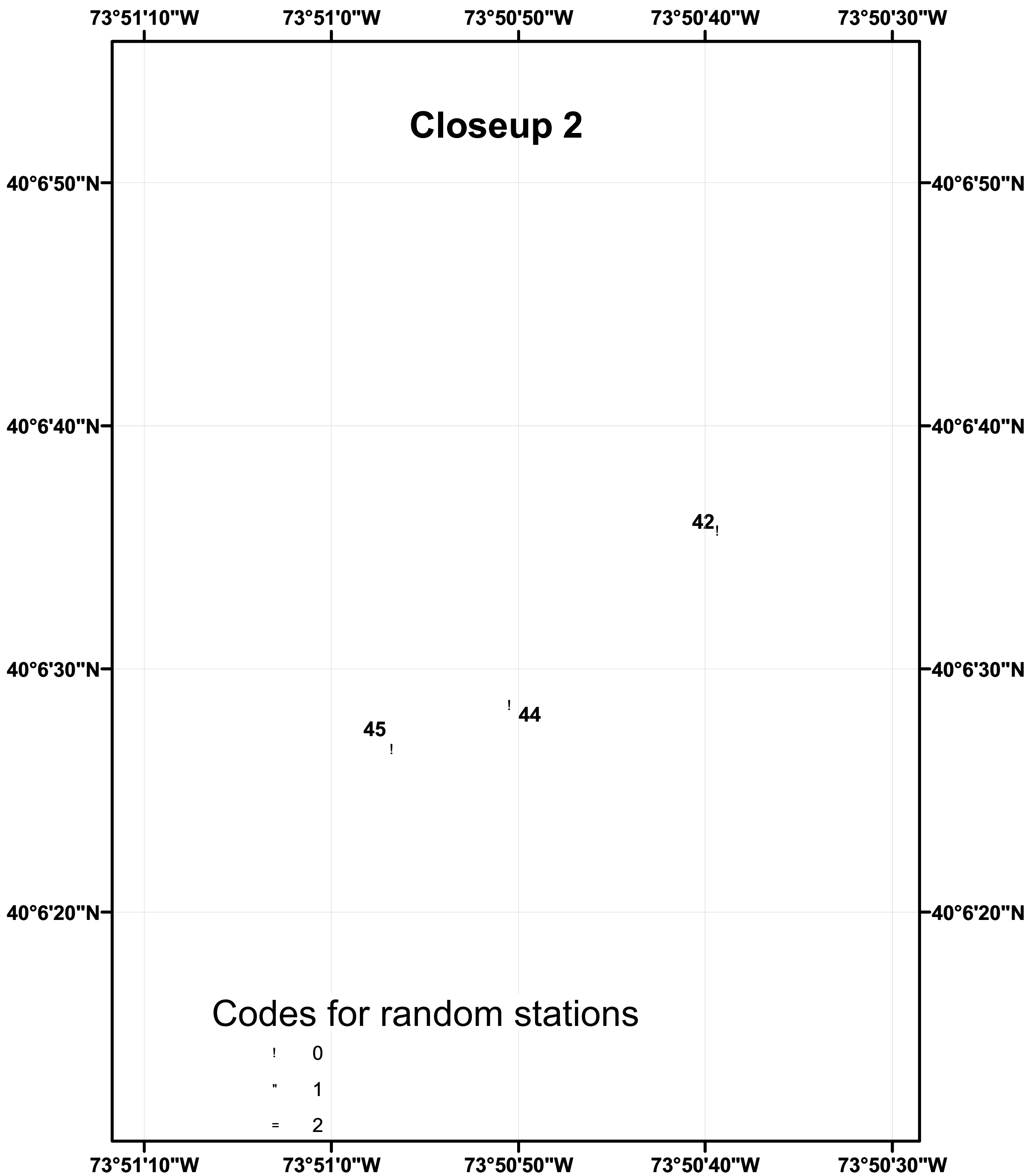

Figure C19 (continued)

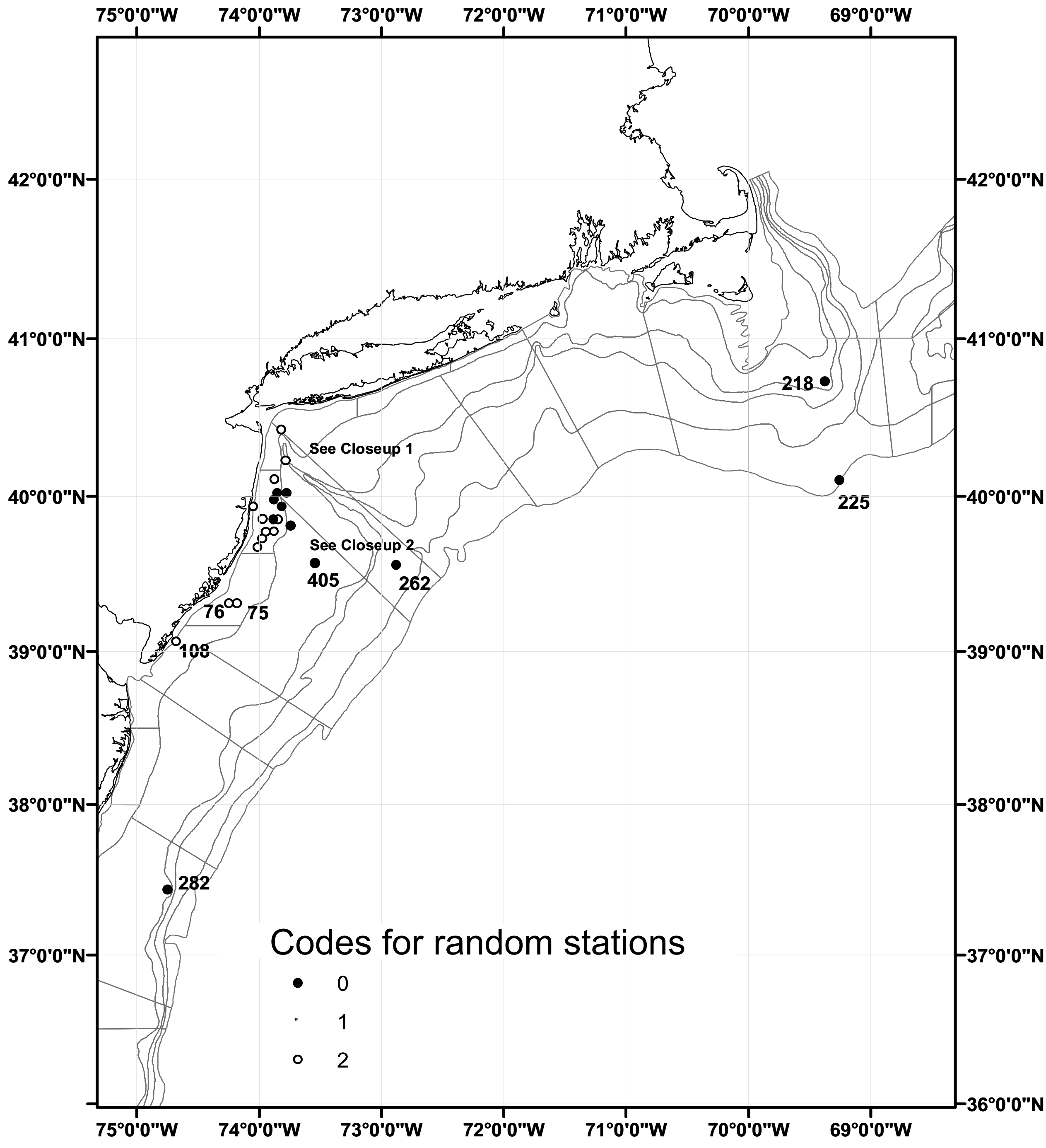

Figure C20. Locations of 2005 survey stations with poor dredge performance that would not have been excluded from trend and swept area trend analyses based on haul or gear damage codes, with station numbers. Codes 1 and 2 (dark squares and open circles) are random stations. Stations in close-up 2 are all from a depletion experiment.

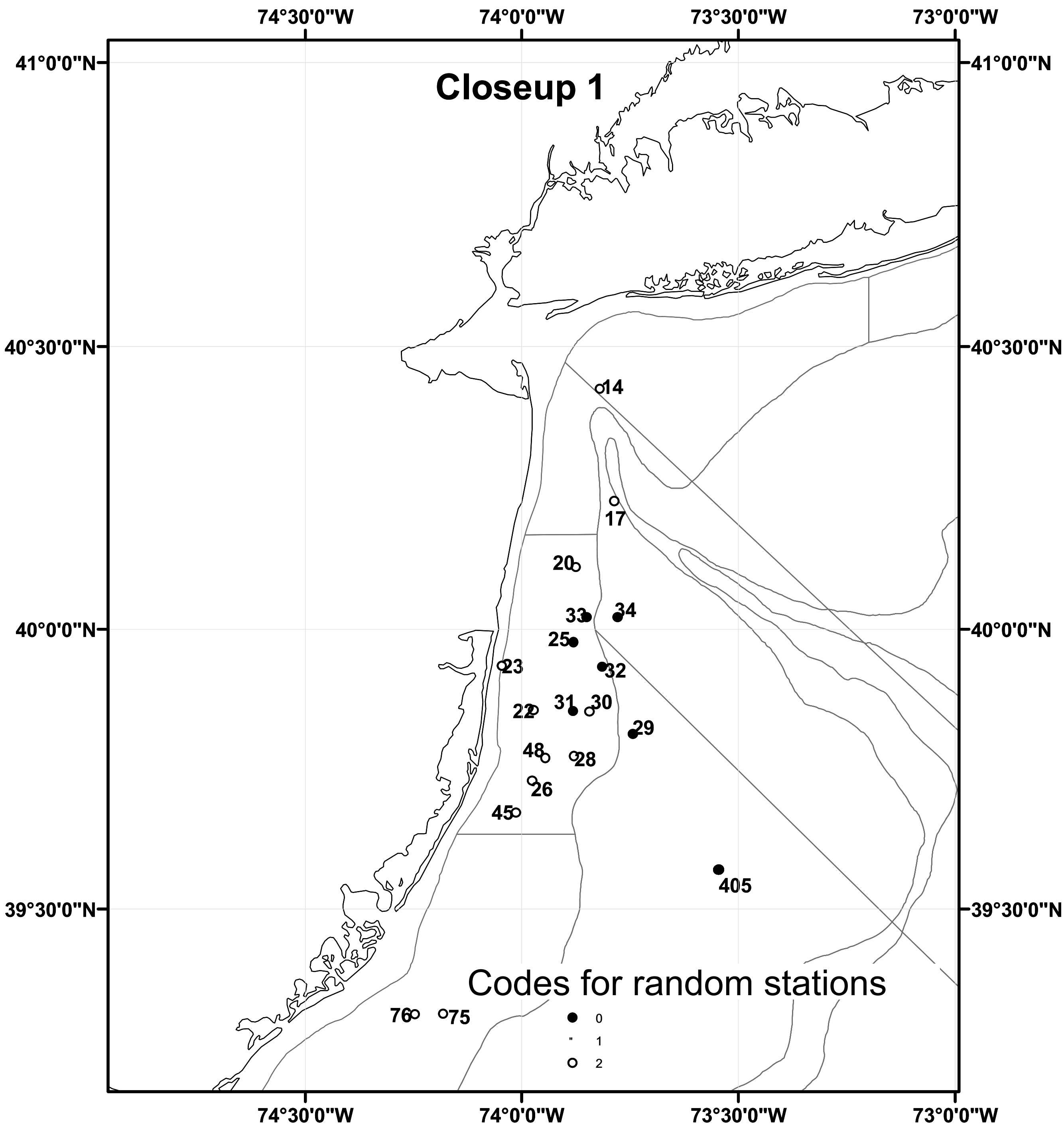

Figure C20 (continued)

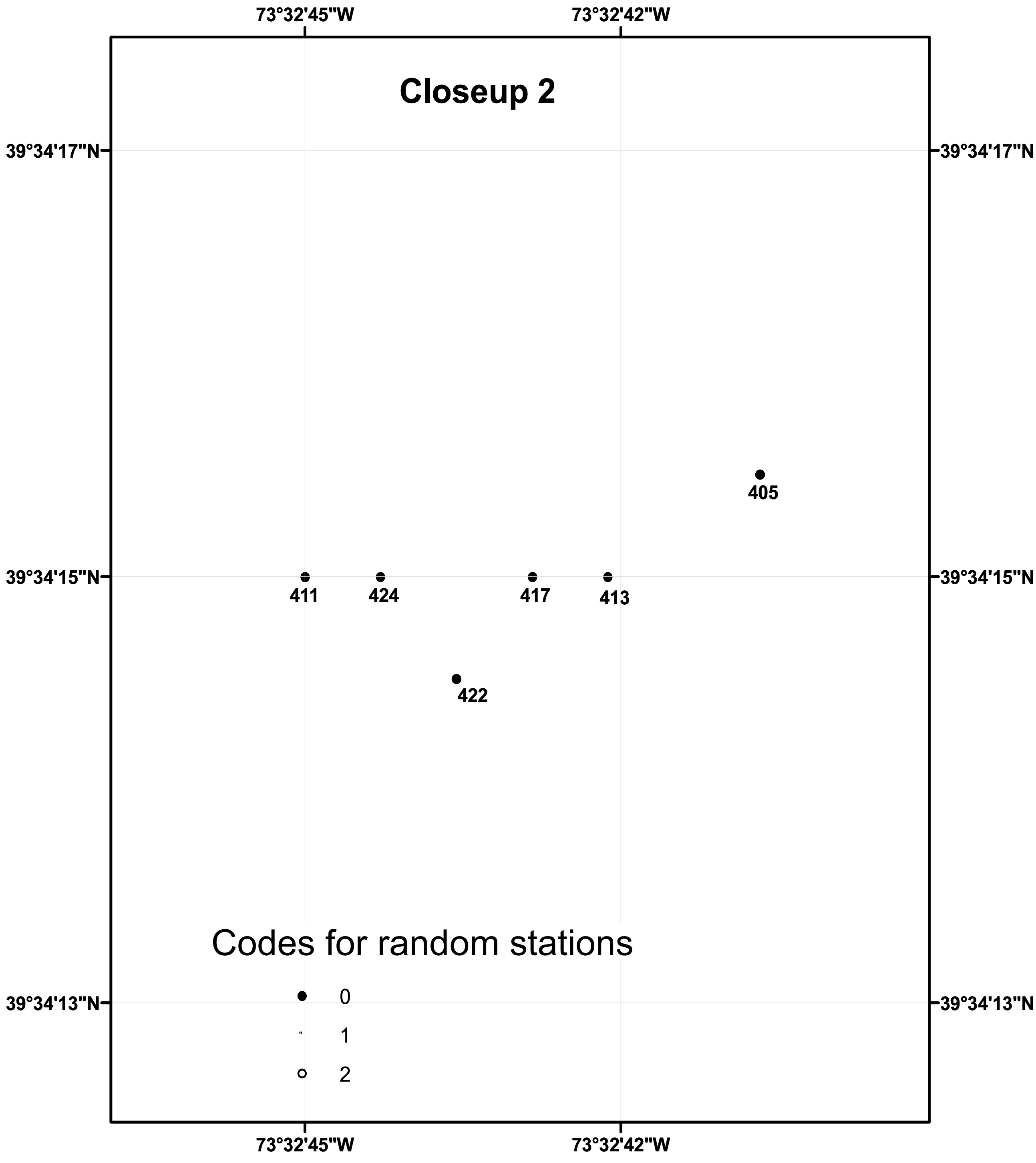

Figure C20 (continued)

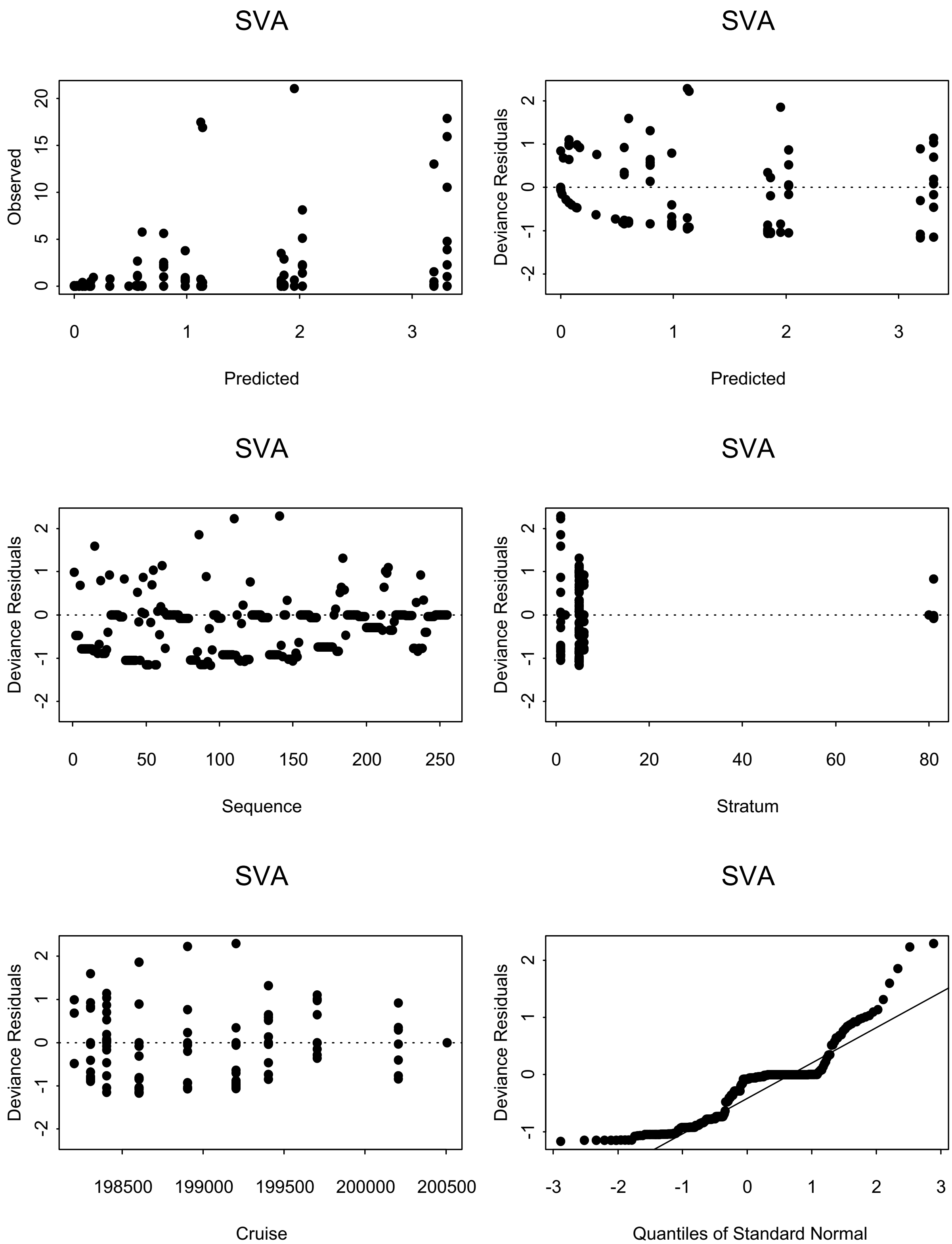

Figure C21. Residuals and diagnostics for negative binomial GLM model used to impute missing survey data for surfclam in SVA.

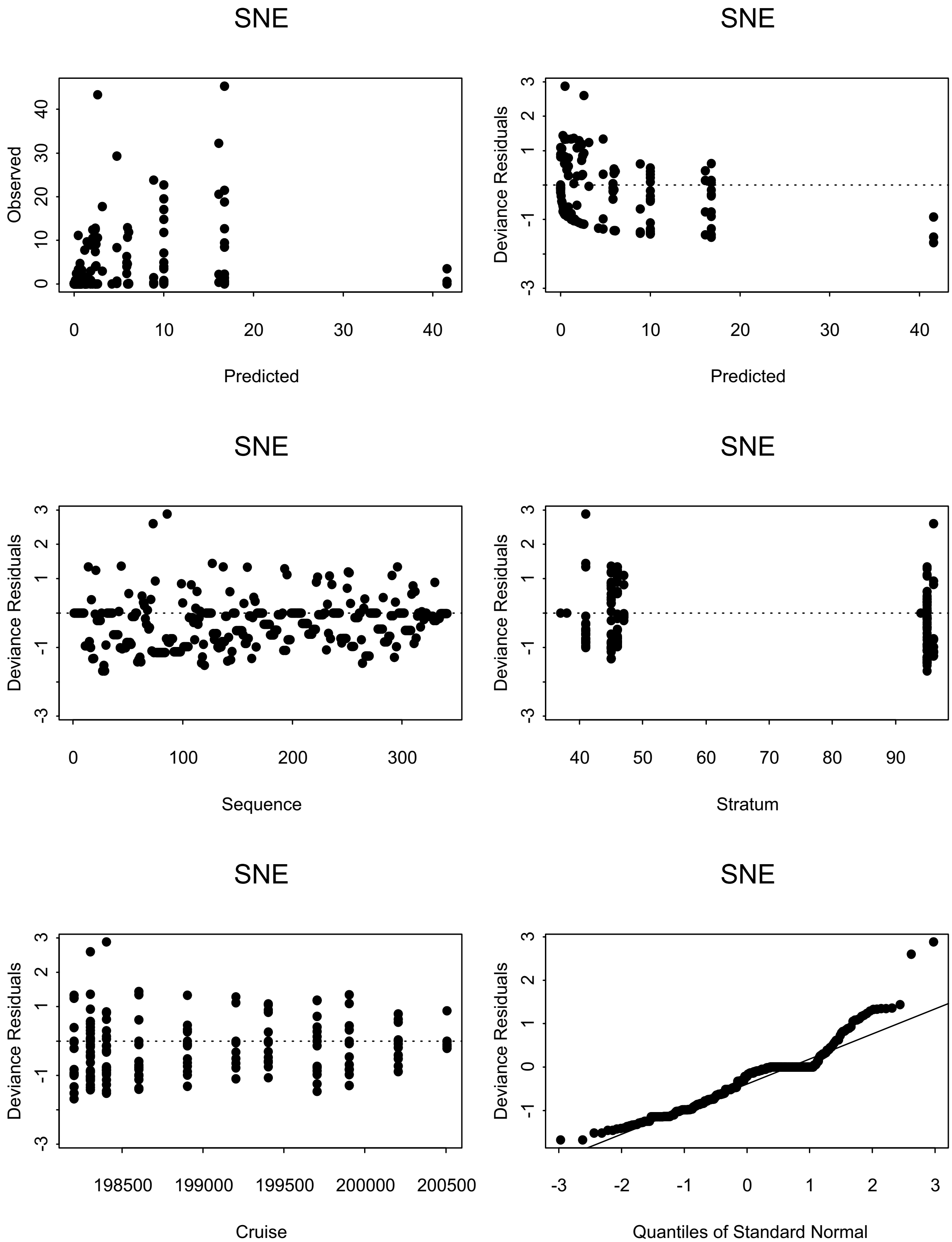

Figure C22. Residuals and diagnostics for negative binomial GLM model used to impute missing survey data for surfclam in SNE.

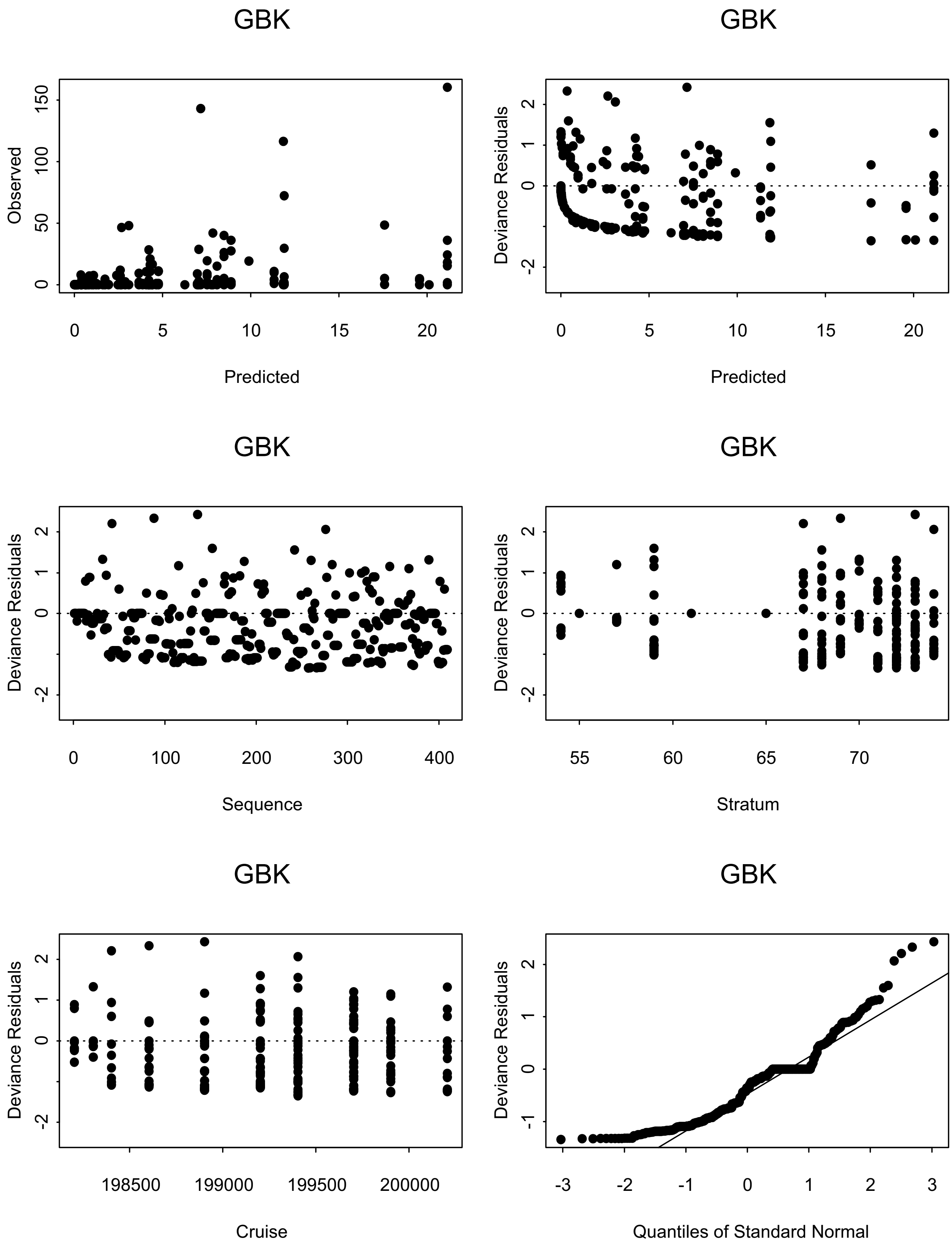

Figure C23. Residuals and diagnostics for negative binomial GLM model used to impute missing survey data for surfclam in GBK.

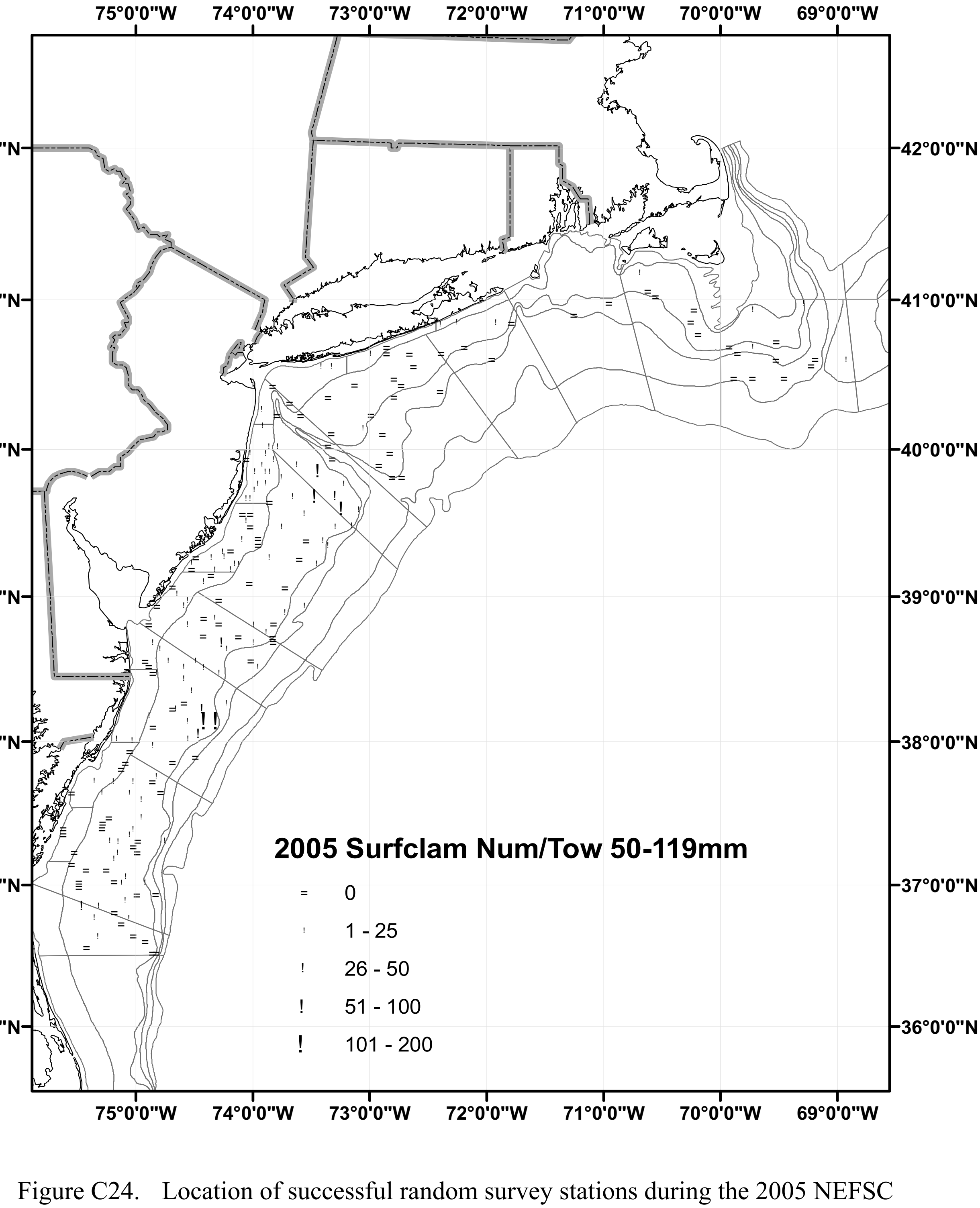

Figure C24. Location of successful random survey stations during the 2005 NEFSC clam survey with catches for small recruit surfclam 80-119 mm SL. Catches are numbers per tow, standardized by doppler distance with no borrowing.

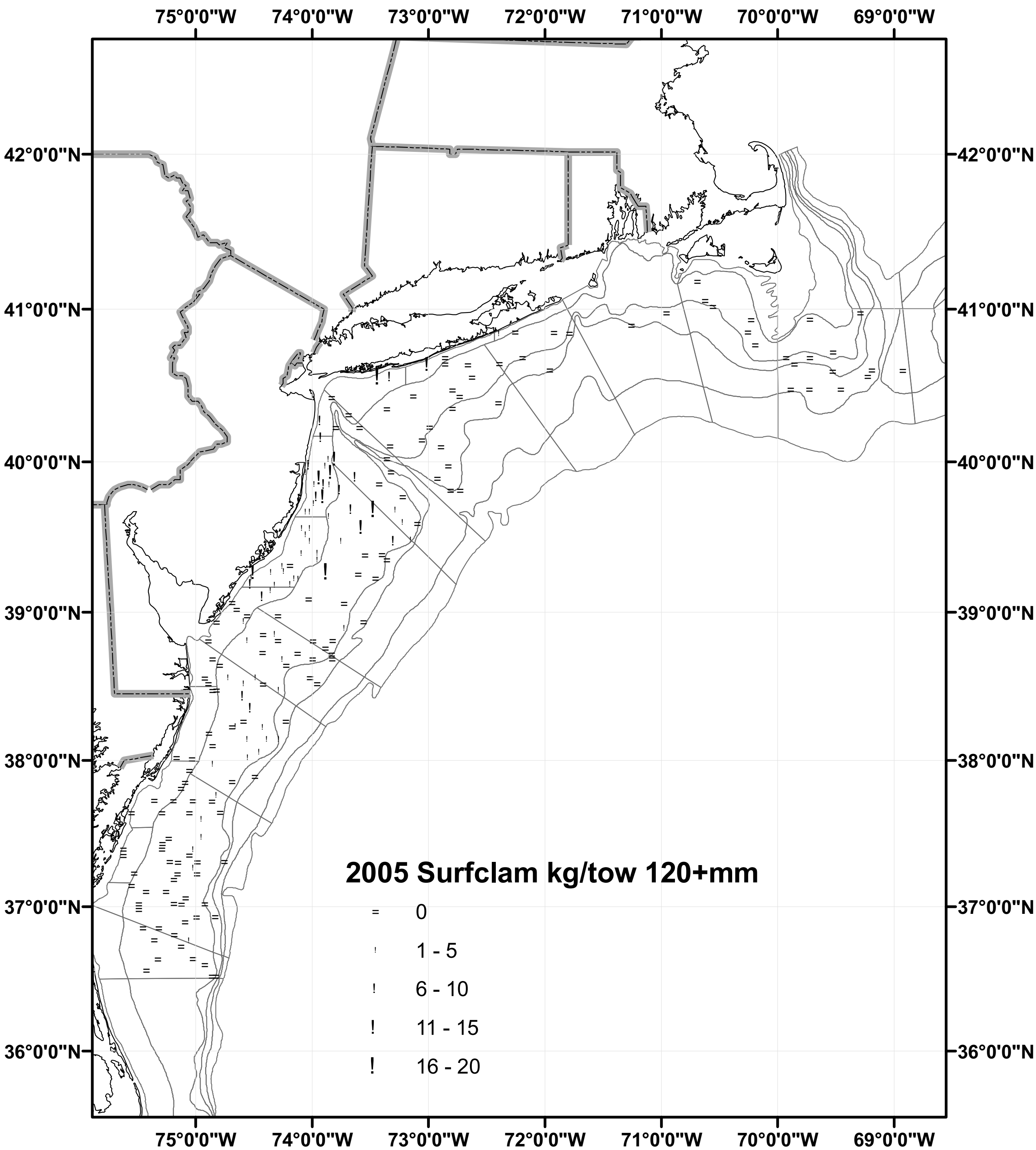

Figure C25. Location of successful random survey stations during the 2005 NEFSC clam survey with catches for large fishable surfclam 120+ mm SL. Catches are numbers per tow, standardized by doppler distance with no borrowing.

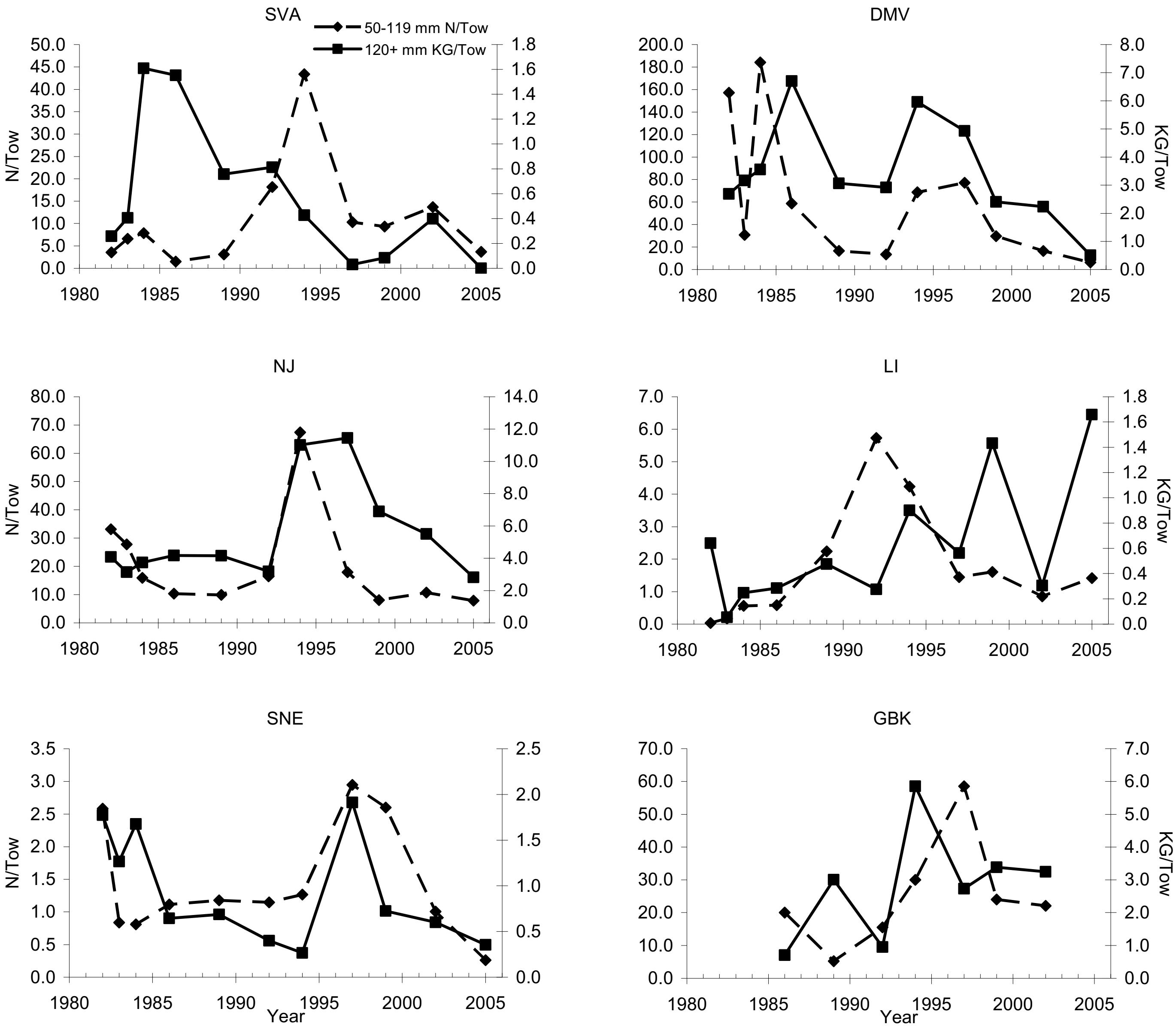

Figure C26. Trends in abundance (mean n tow^{-1}) for small recruit surfclam (50-119 mm) and trends in biomass (mean kg tow^{-1}) for large fishable (120+ mm) surfclam based on NEFSC clam surveys, by region.

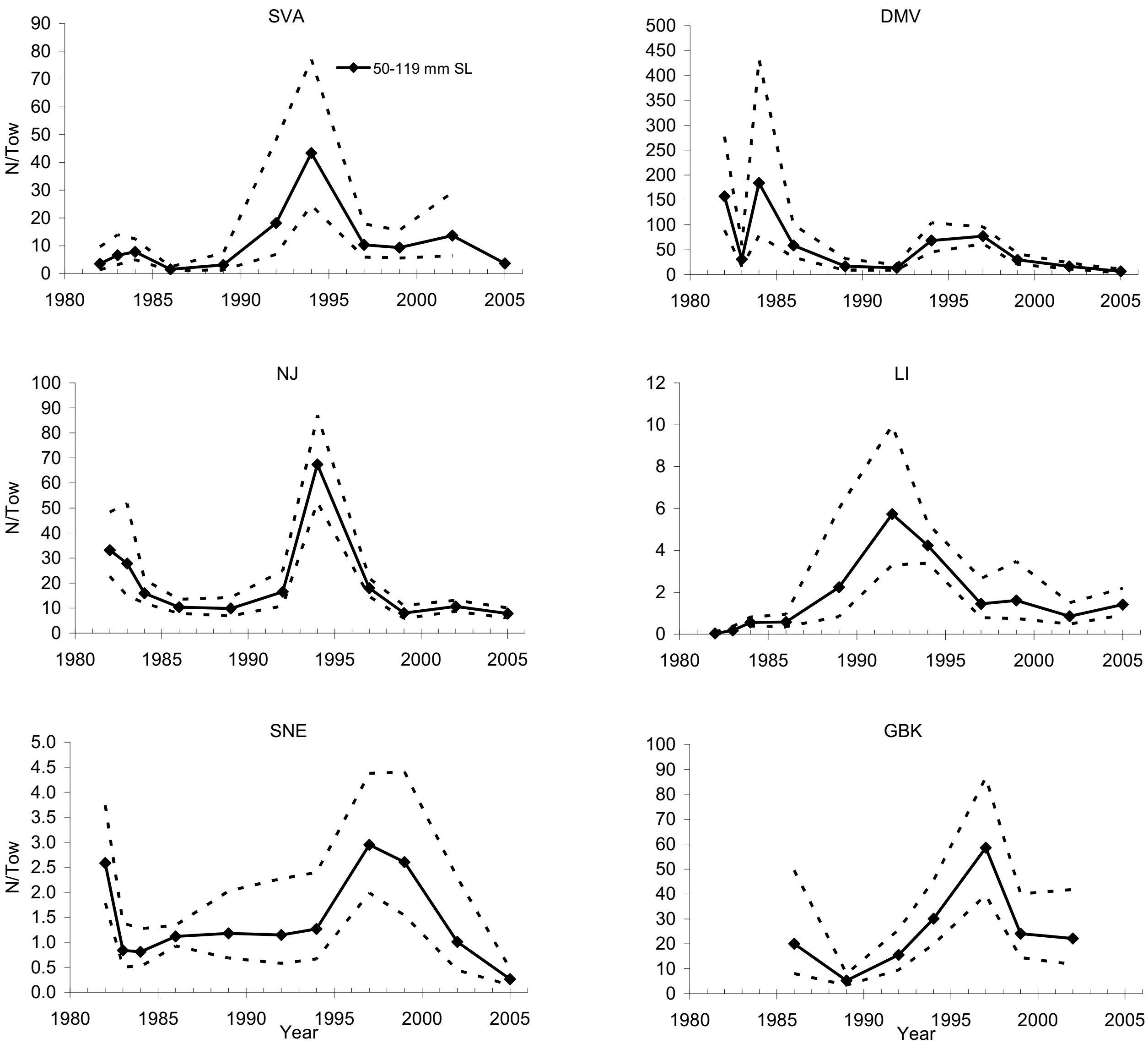

Figure C27. Trends in abundance indices (mean n tow^{-1}) for small recruit surfclam (50-119 mm SL) in NEFSC clam surveys, with 80% confidence intervals assuming lognormal measurement errors and arithmetic CVs for stratified random sampling based on Students-*t* distribution with the number of tows as degrees of freedom.

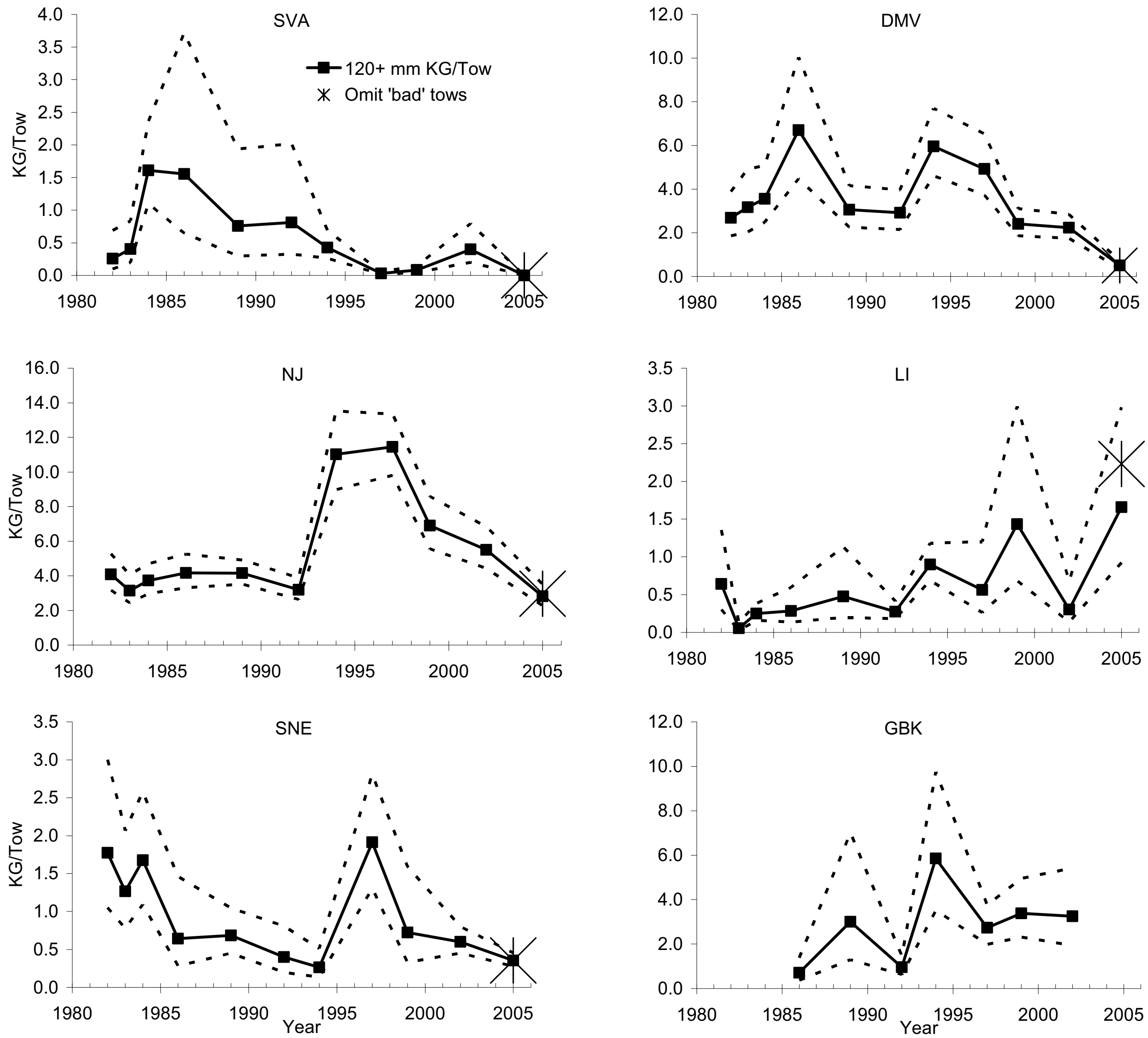

Figure C28. Trends in biomass indices (mean kg tow^{-1}) for large fishable surfclam (120+ mm SL) in NEFSC clam surveys, with 80% confidence intervals assuming lognormal measurement errors and arithmetic CVs for stratified random sampling based on Students-*t* distribution with the number of tows as degrees of freedom. Different symbols show effects of omitting tows with poor gear performance during 2005.

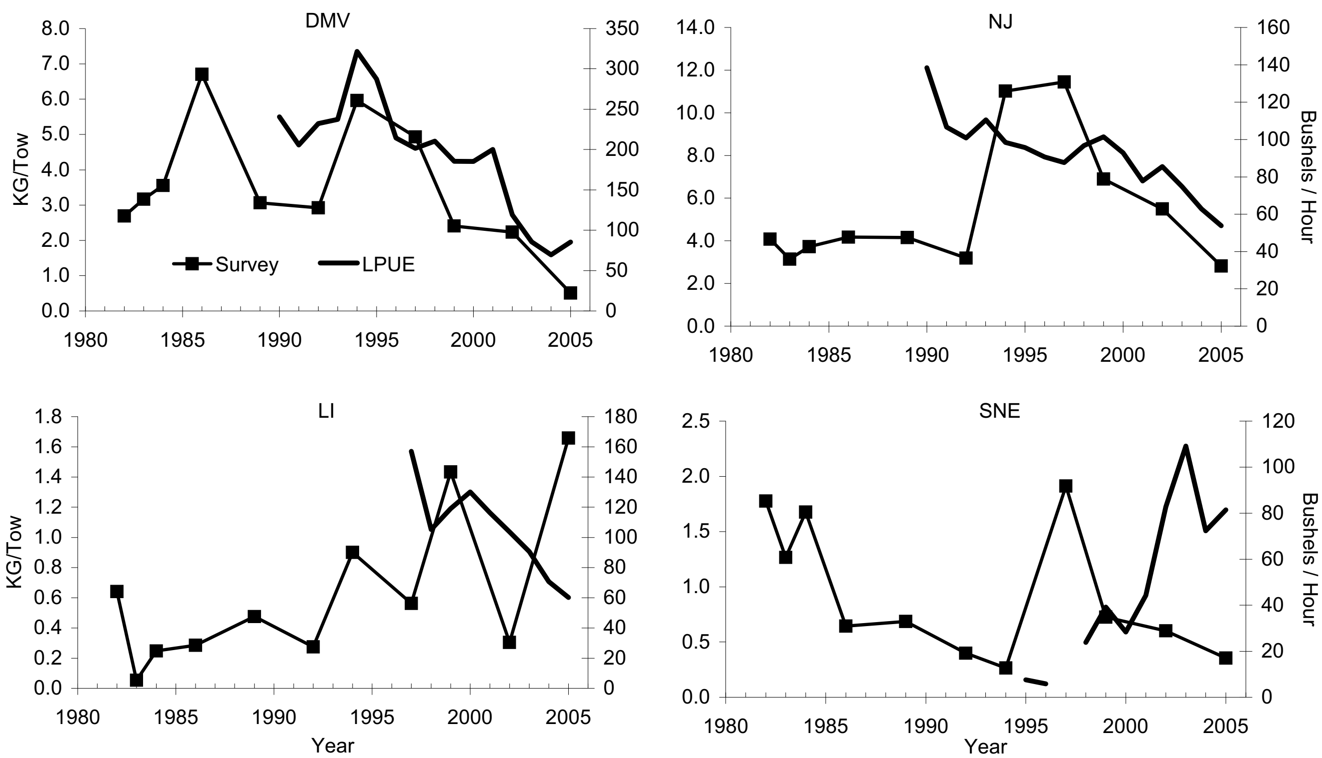

Figure C29. Trends in biomass indices for large fully large surfclam (mean kg tow^{-1}, 120+ mm SL) in NEFSC clam surveys and standardized LPUE in the commercial fishery.

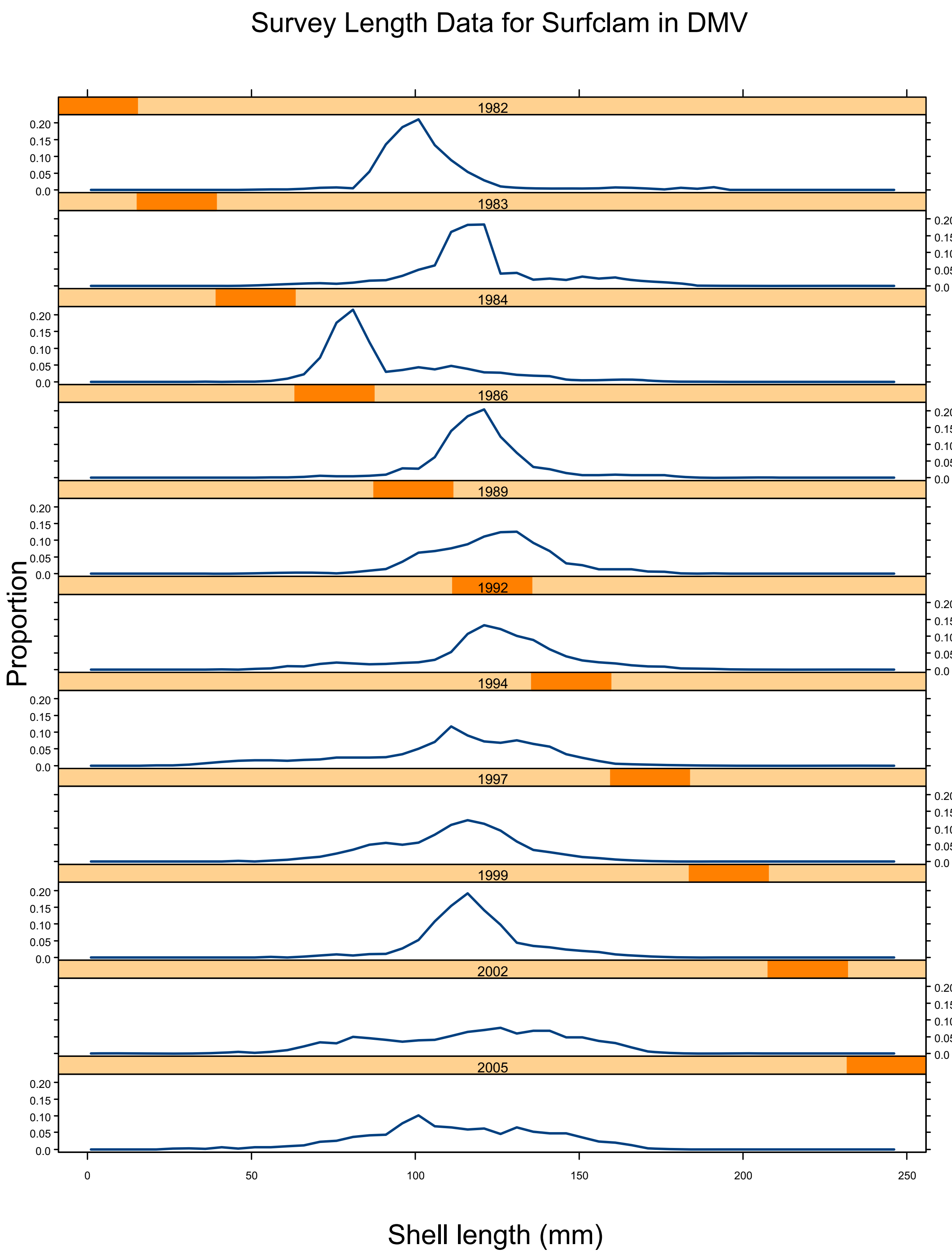

Figure C30. Survey length composition data for surfclam in the DMV region.

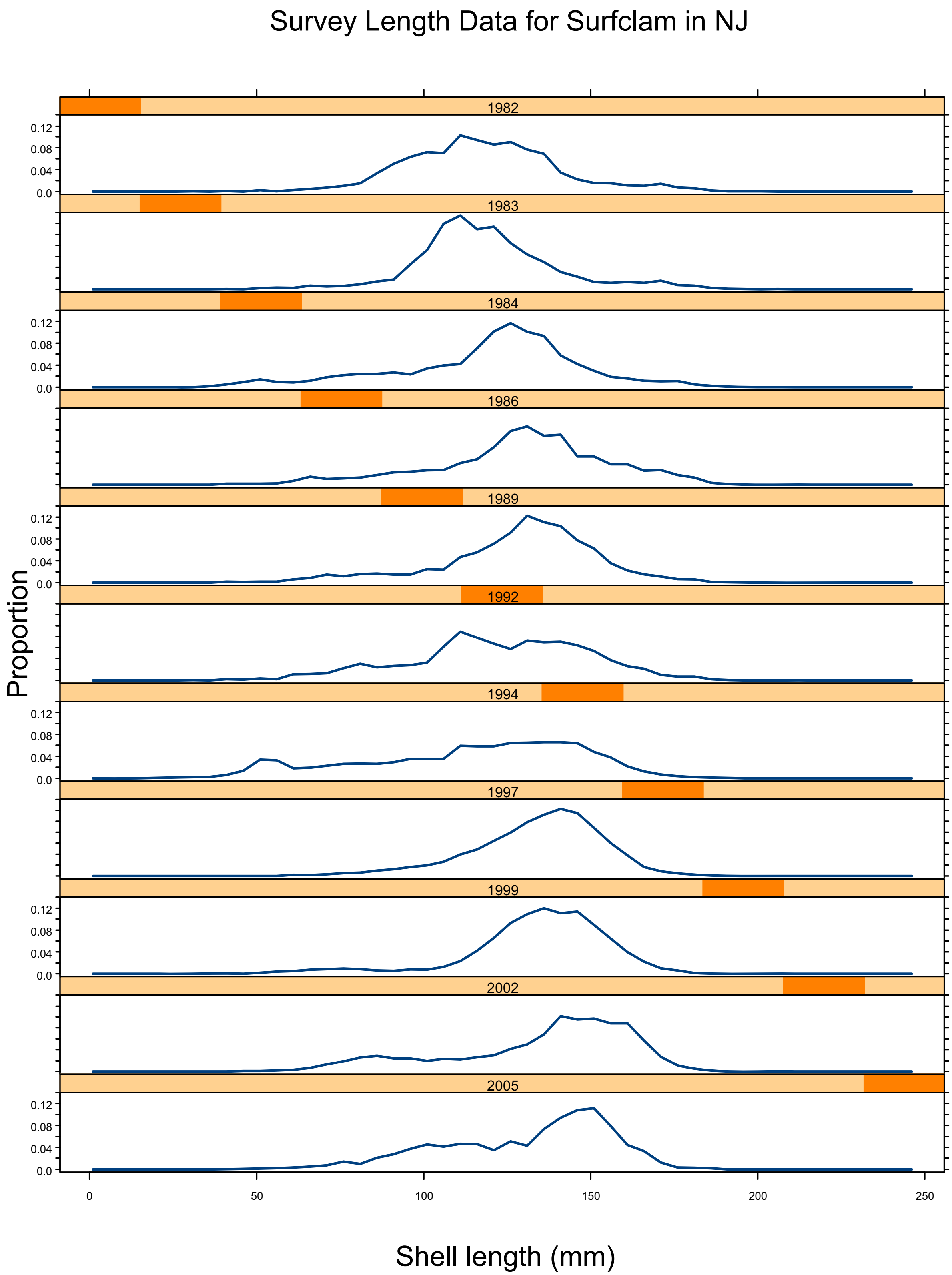

Figure C31. Survey length composition data for surfclam in the NJ region.

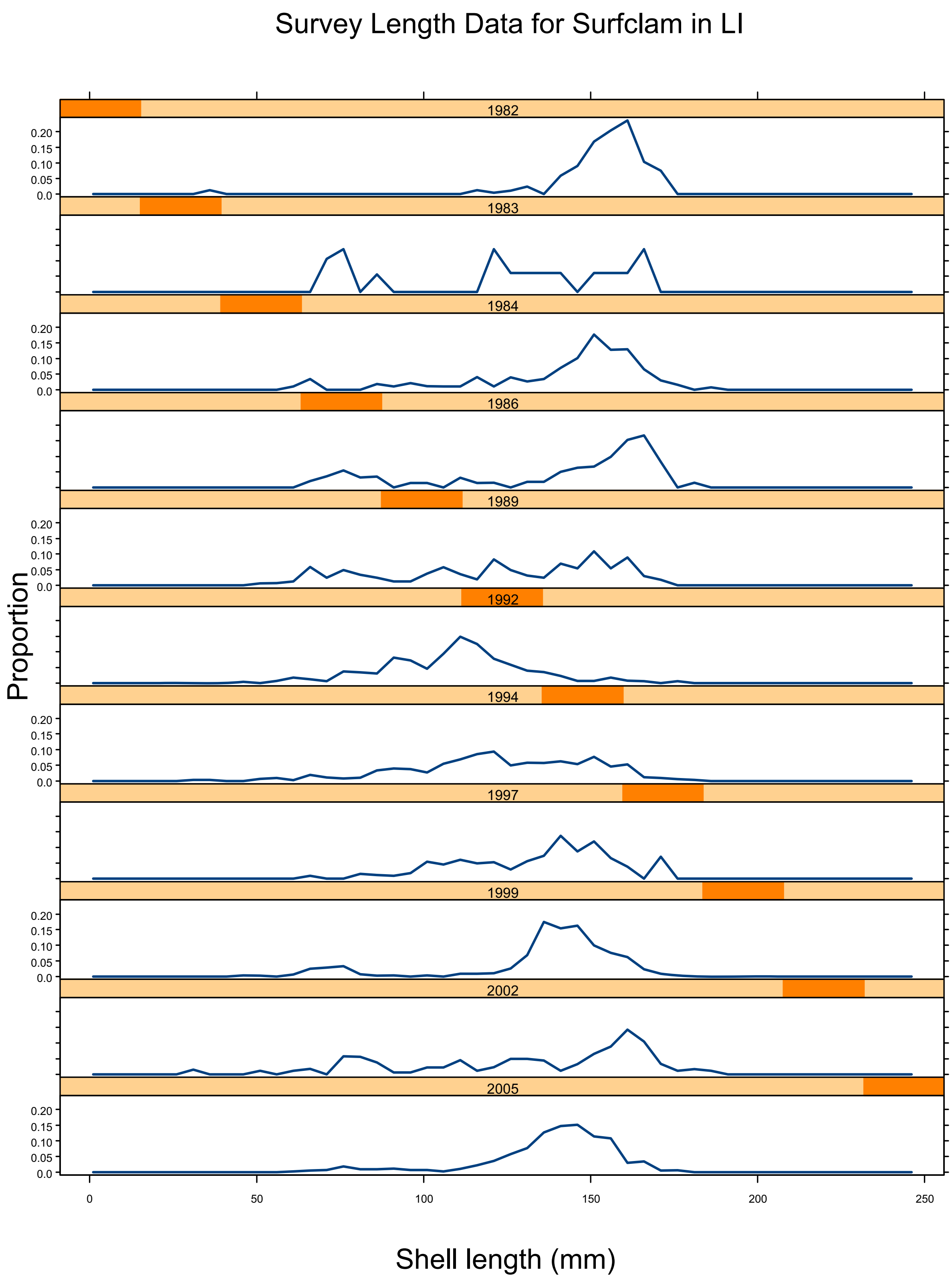

Figure C32. Survey length composition data for surfclam in the LI region.

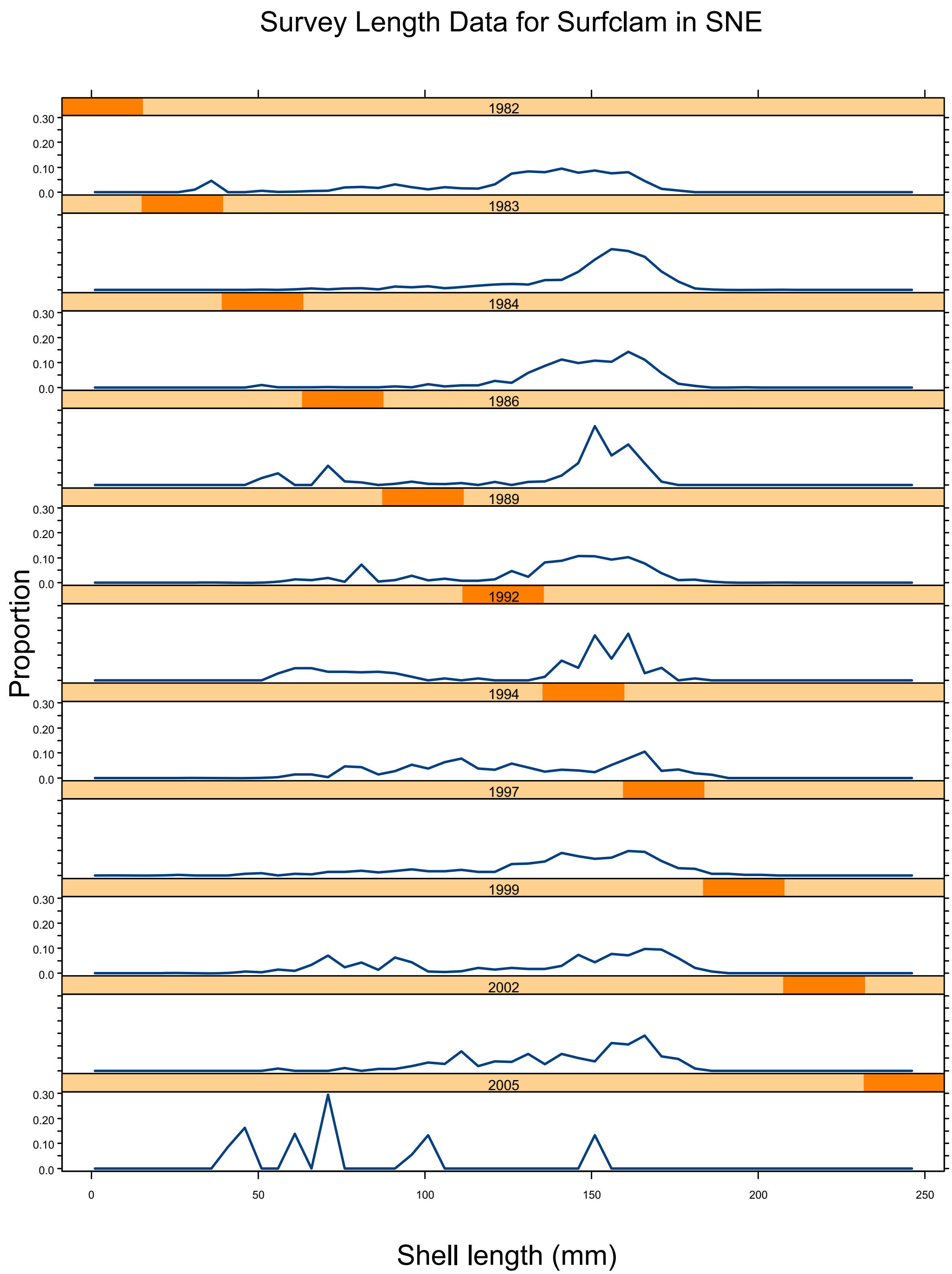

Figure C33. Survey length composition data for surfclam in the SNE region.

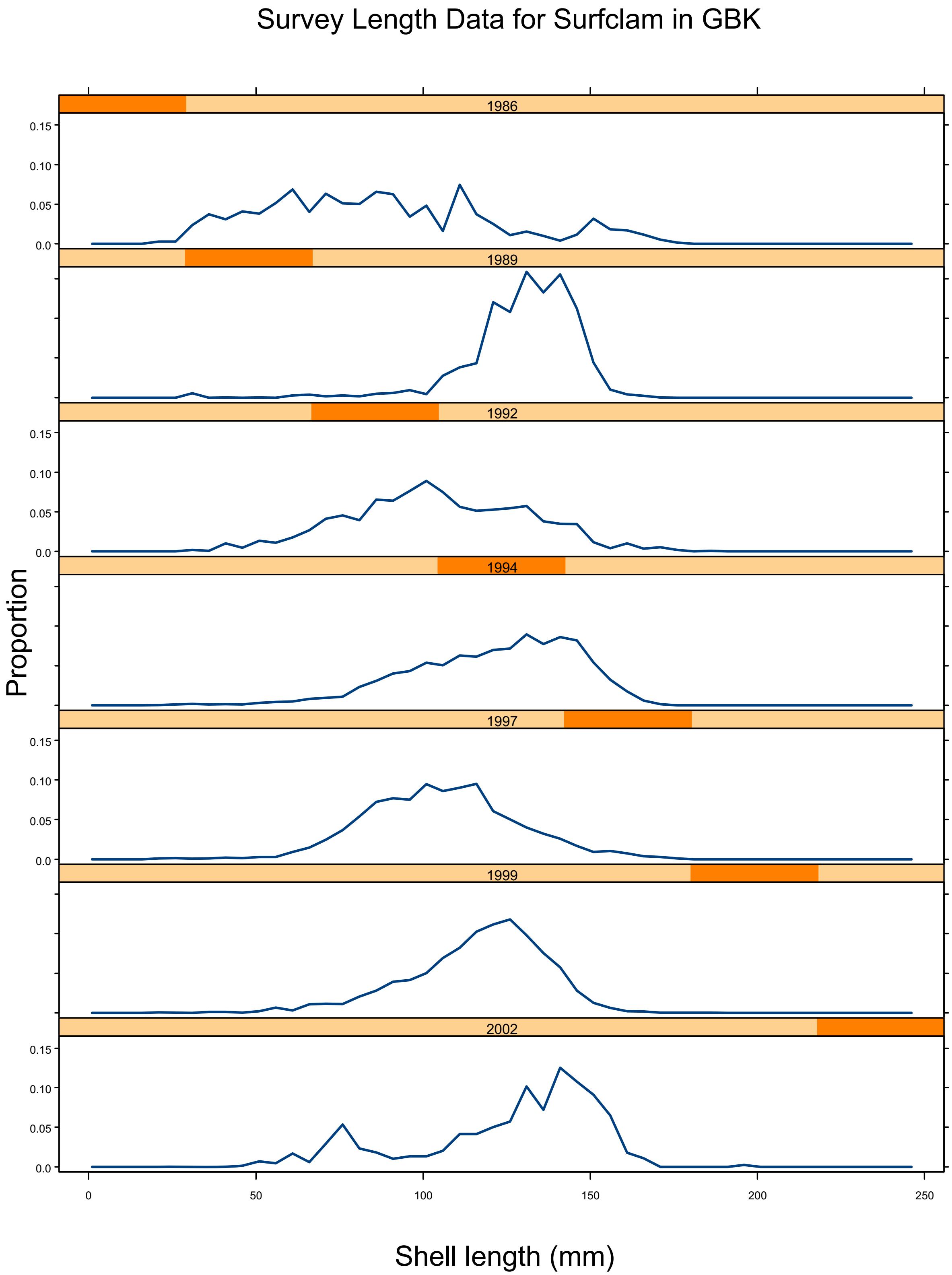

Figure C34a. Survey length composition data for surfclam in the GBK region.

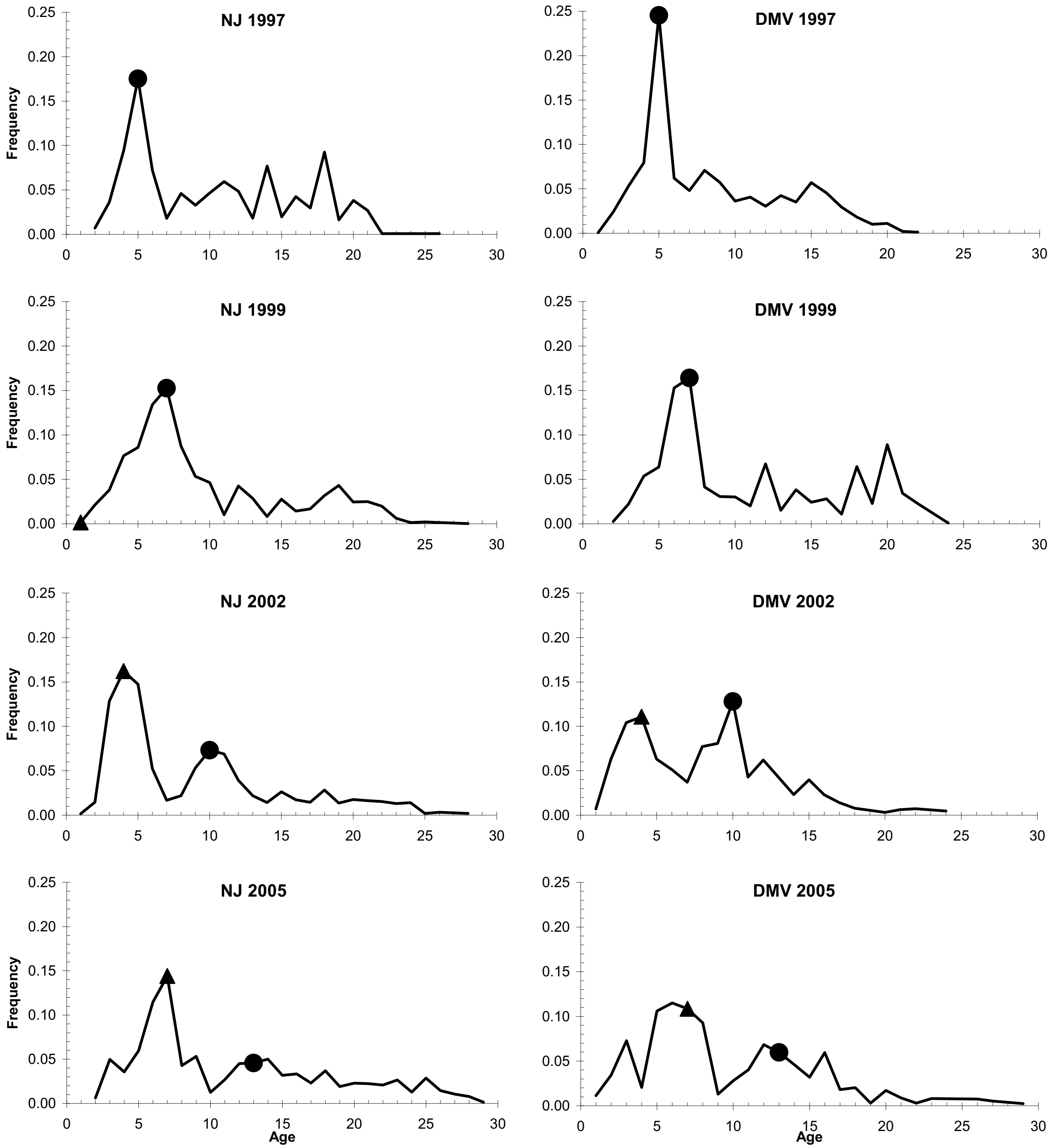

Figure 34b. NEFSC clam survey age composition data for surfclam in the NJ and DMV areas during 1997-2005. There is uncertainty about the timing of annual ring formation. Assuming rings form during the fall after the NEFSC clam survey, dark circles identify the 1992 year class (14 rings in 2005) and dark triangles identify the 1999 year class (7 rings in 2005).

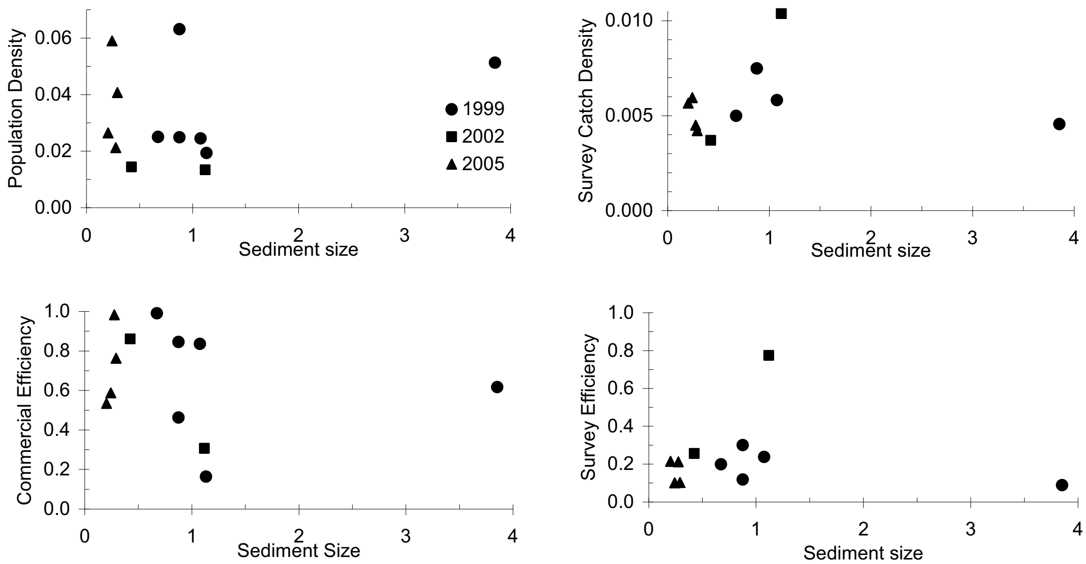

Figure C35. Relationships between depletion study variables and sediment grain size based on depletion studies during 1999, 2002 and 2005. Sediment data were not collected during 1997 and 2004.

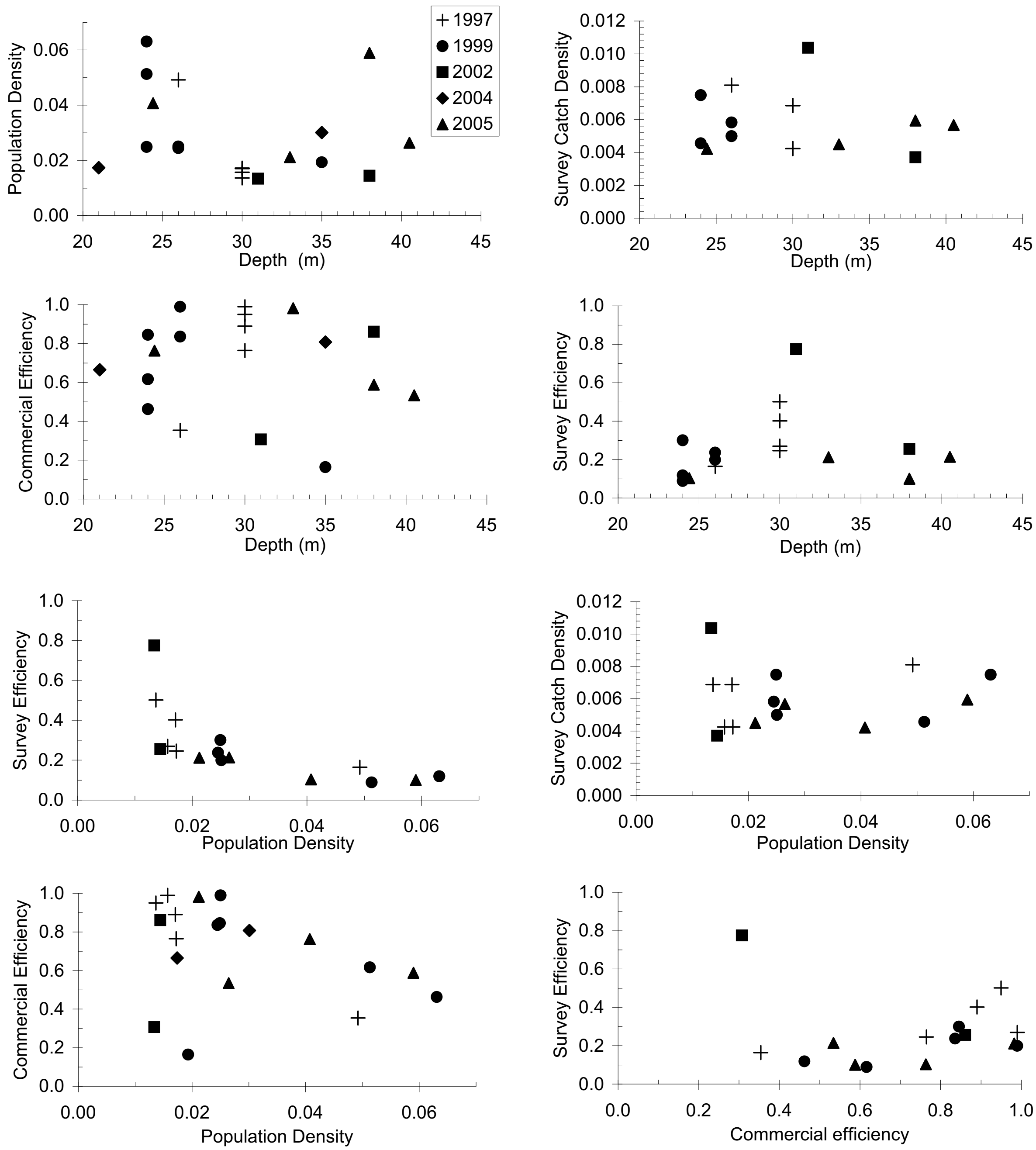

Figure C36. Relationships between depletion study variables based on all depletion studies during 1997- 2005.

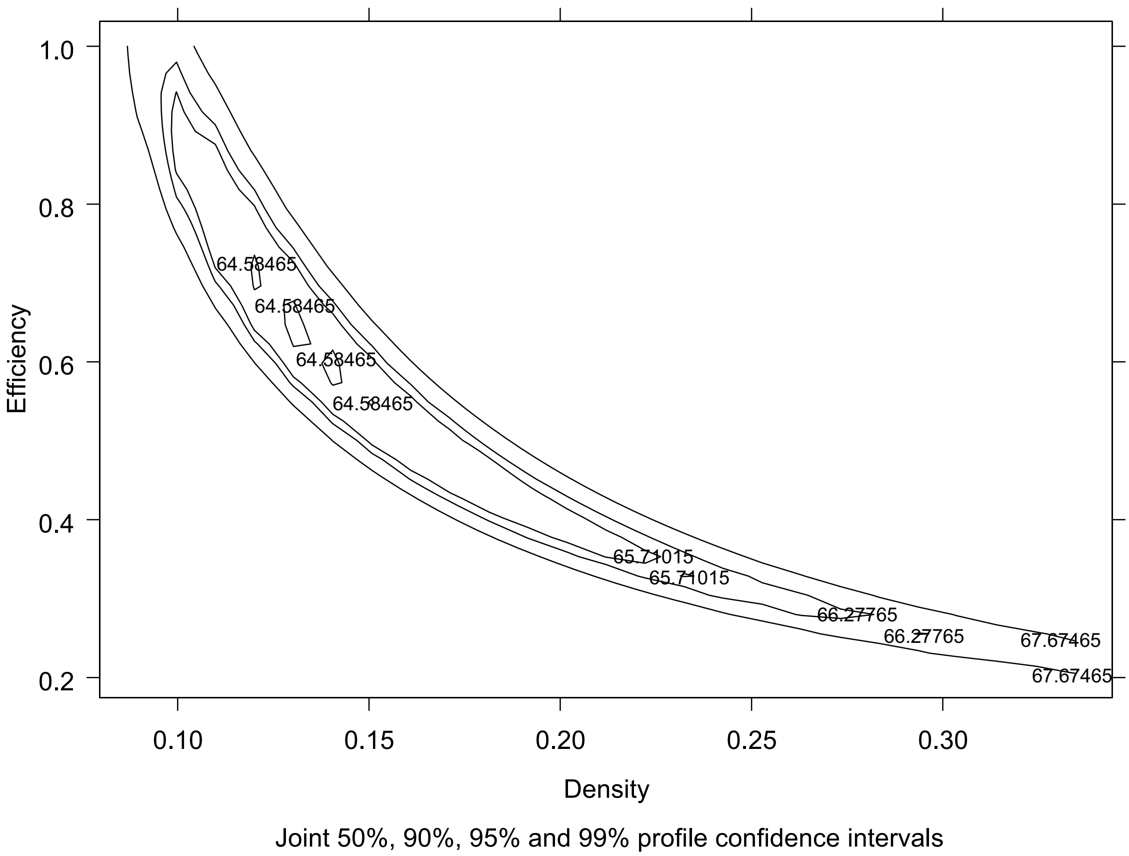

Figure C37. Likelihood profile analysis for efficiency and density estimates from the Patch model for the SC1999-7 surfclam depletion experiment. The joint 50% confidence interval for efficiency and density is the area within the outermost contour. The joint 99% confidence interval is the area inside the innermost contour lines. Contour lines for the joint 90% and 95% confidence intervals lie between.

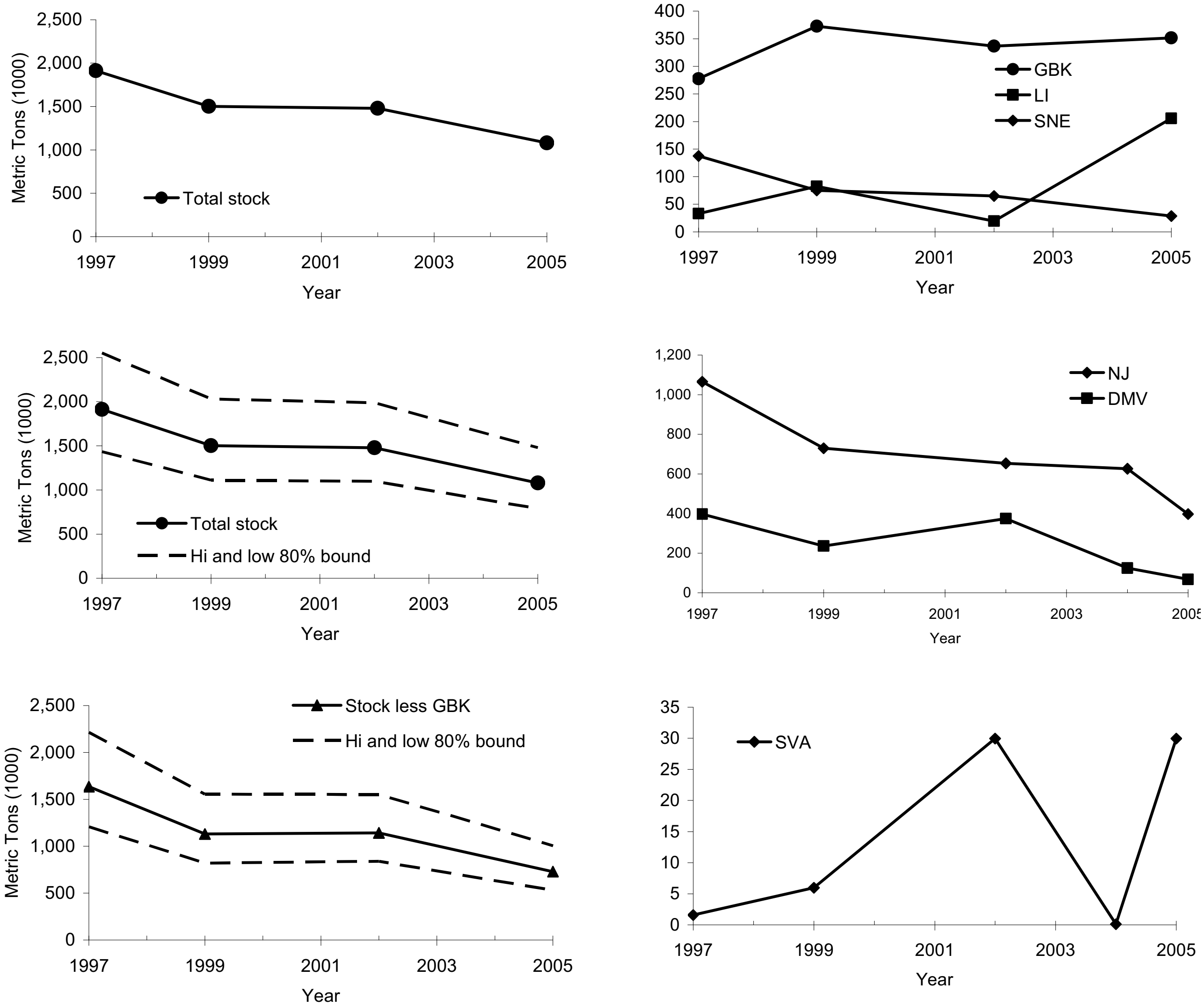

Figure C38. Efficiency corrected swept-area biomass estimates for surfclam 120+ mm SL, including estimates from the 2004 cooperative survey and NEFSC clam surveys during 1997, 1999, 2002 and 2005.

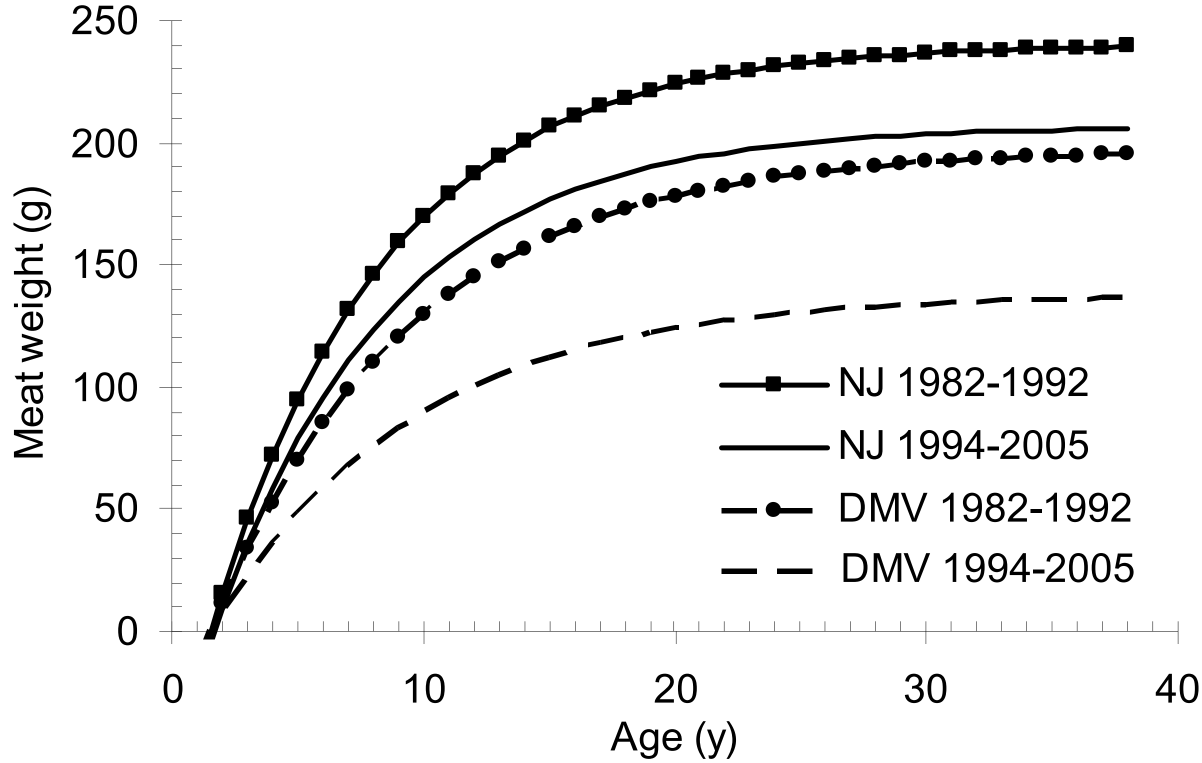

Figure C39. Von Bertlanffy curves for size (meat weight) at age of surfclam during 1982-1992 and 1994-2005 in the NNJ and DMV regions, based on NEFSC clam survey data for 1982-2005.

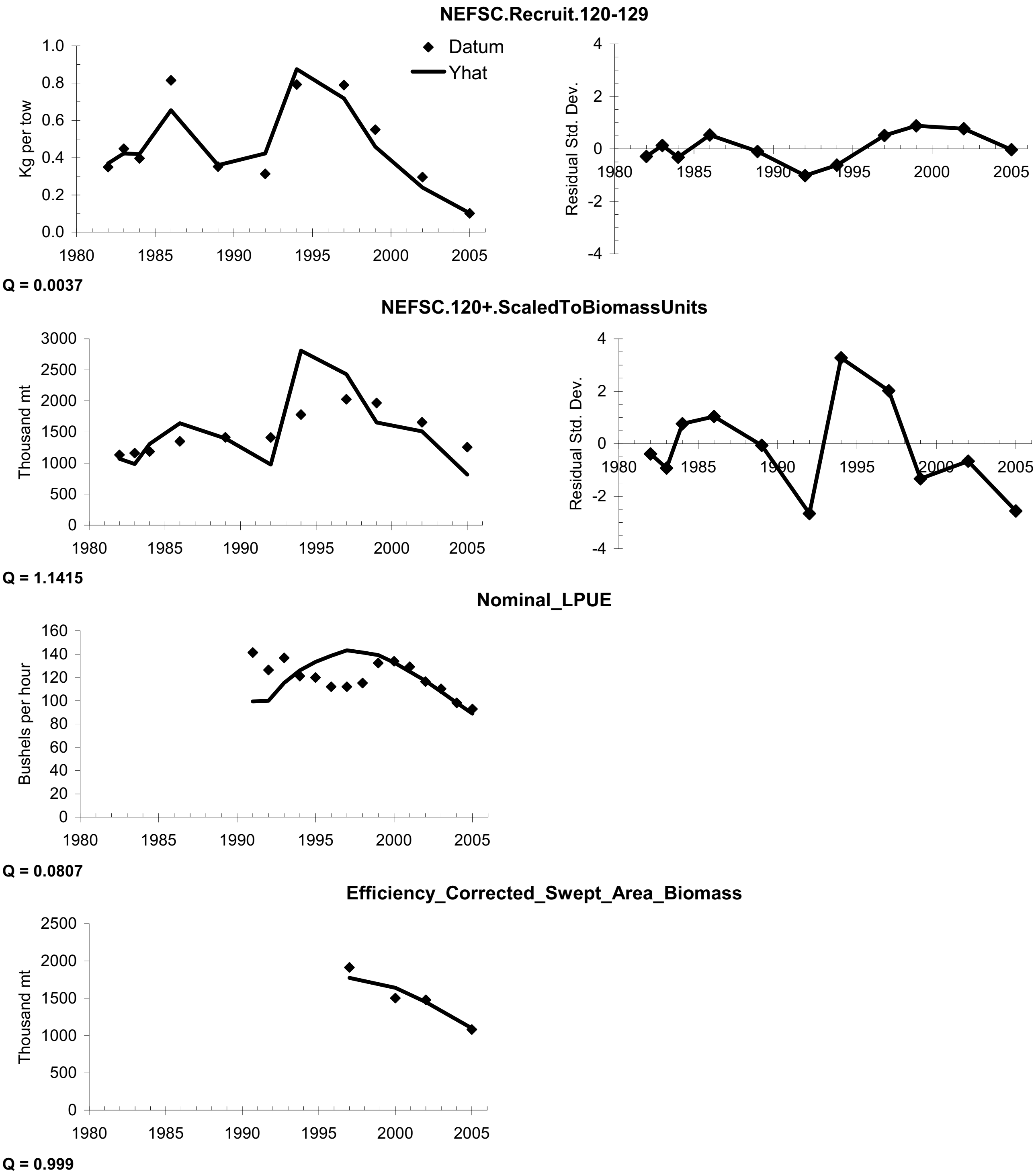

Figure C40. Model diagnostics for the KLAMZ model for the entire stock of surfclam. Trends in nominal LPUE and efficiency corrected swept area biomass are shown with predicted trends from the model for comparison, but trends in these indices did not affect model estimates. Survey scaling parameter (*Q*) estimates are shown below plots for each set of data.

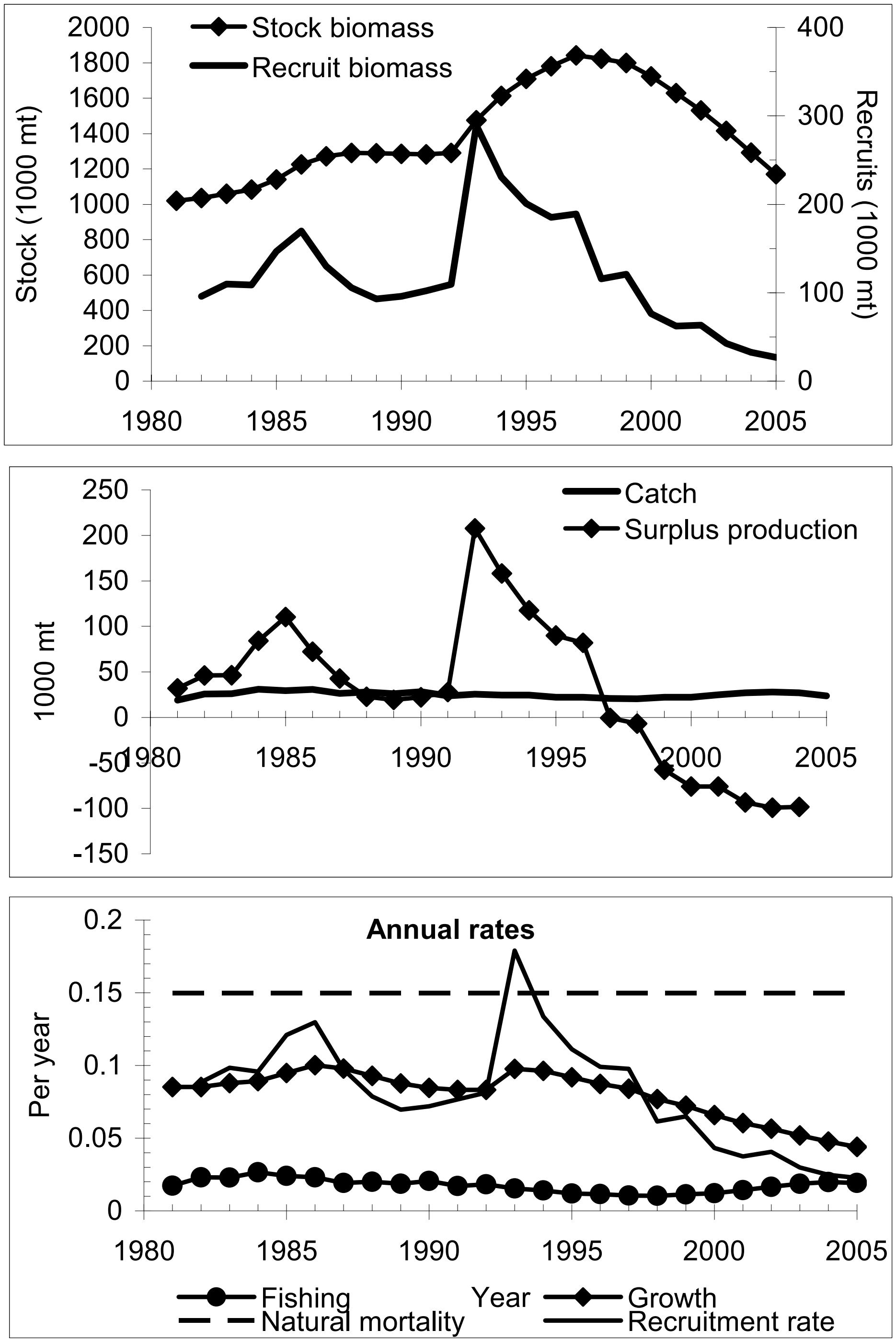

Figure C41. Population dynamics estimates from the KLAMZ model for the entire surfclam stock.

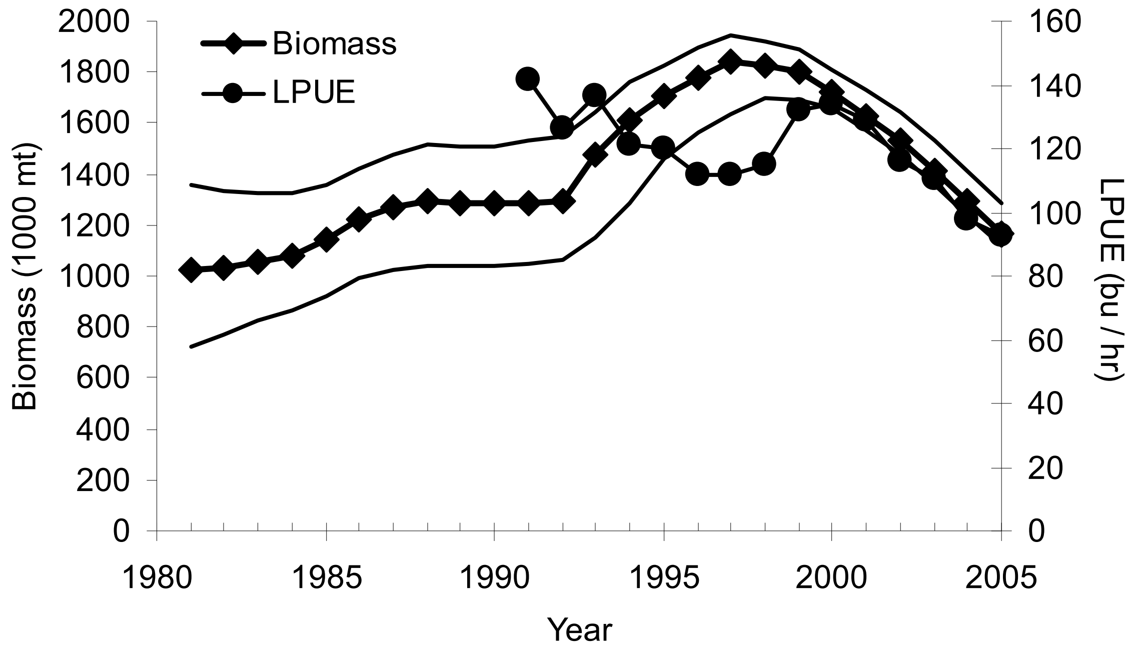

Figure C42. Fishable biomass estimates with 80% empirical confidence intervals from bootstrapping for the entire surfclam stock. Nominal LPUE from logbooks (total reported landings / total reported hours fished, all vessels and all trips) for the entire fishery is shown for comparison. LPUE data were not used in estimating biomass.

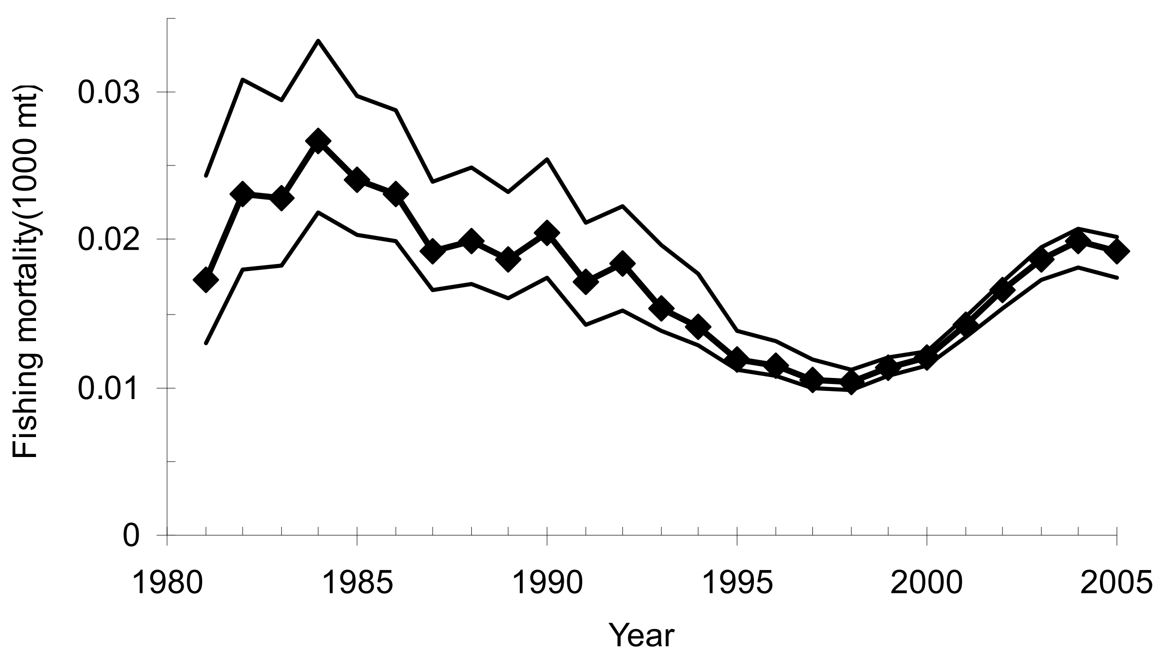

Figure C43. Fishing mortality estimates for the entire surfclam stock with 80% confidence intervals from bootstrapping.

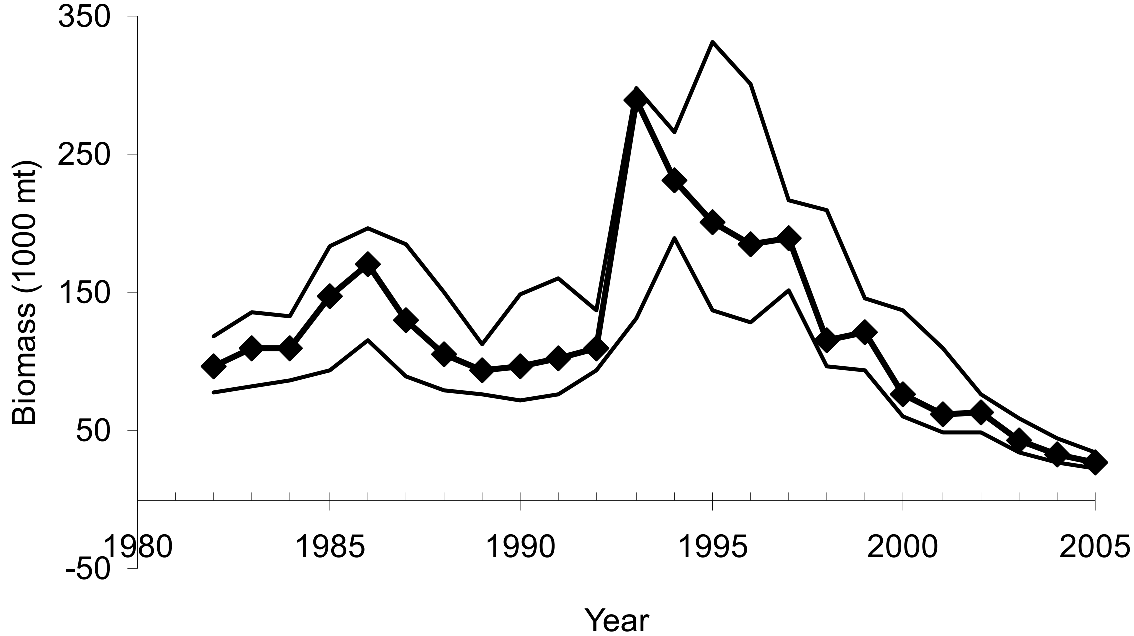

Figure C44. Recruitment for the entire surfclam stock with 80% empirical confidence intervals from bootstrapping.

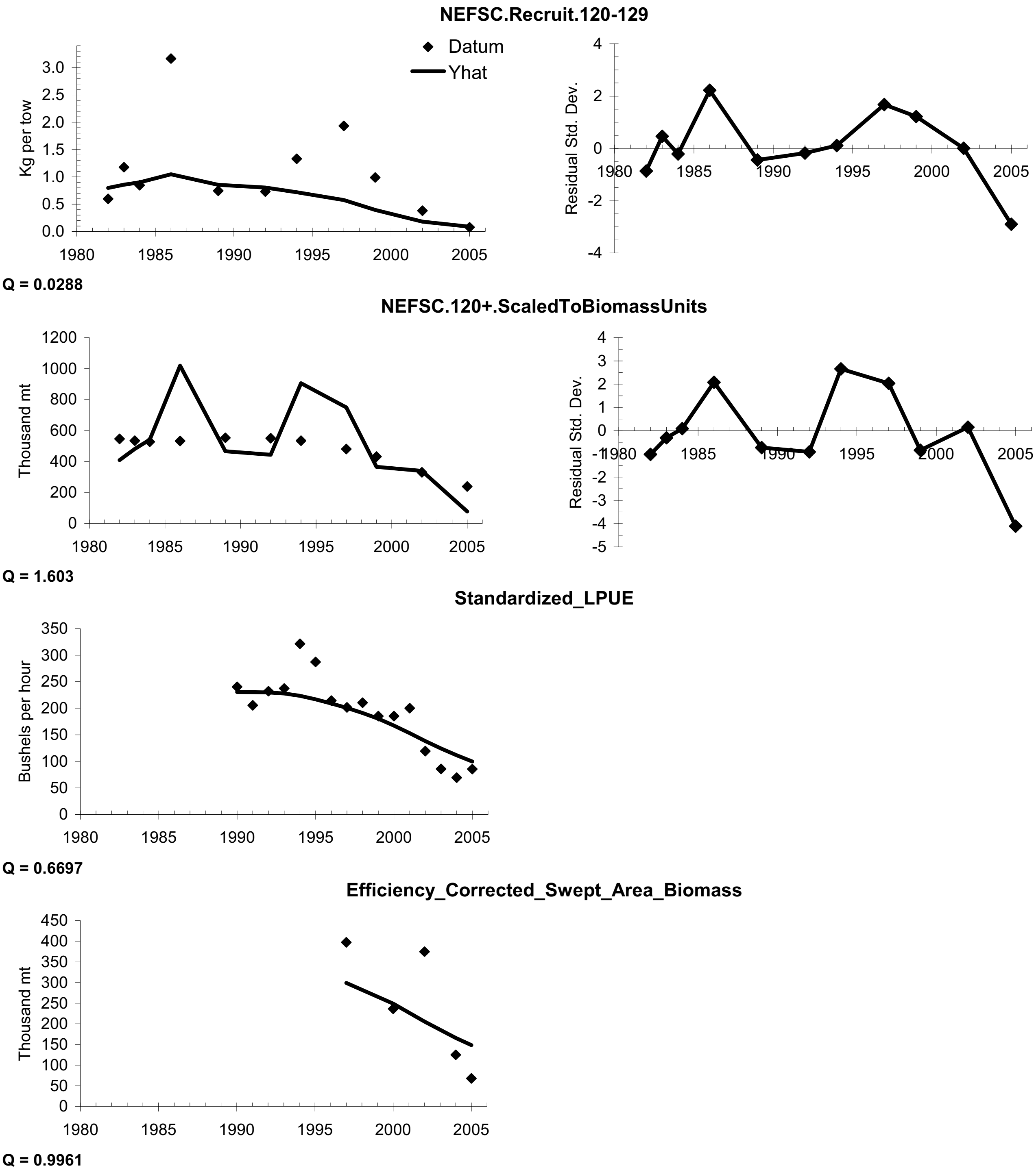

Figure C45. Model diagnostics for the KLAMZ model surfclam in DMV. Trends in nominal LPUE and efficiency corrected swept area biomass are shown with predicted trends from the model for comparison, but trends in these indices did not affect model estimates. Survey scaling parameter (*Q*) estimates are shown below plots for each set of data.

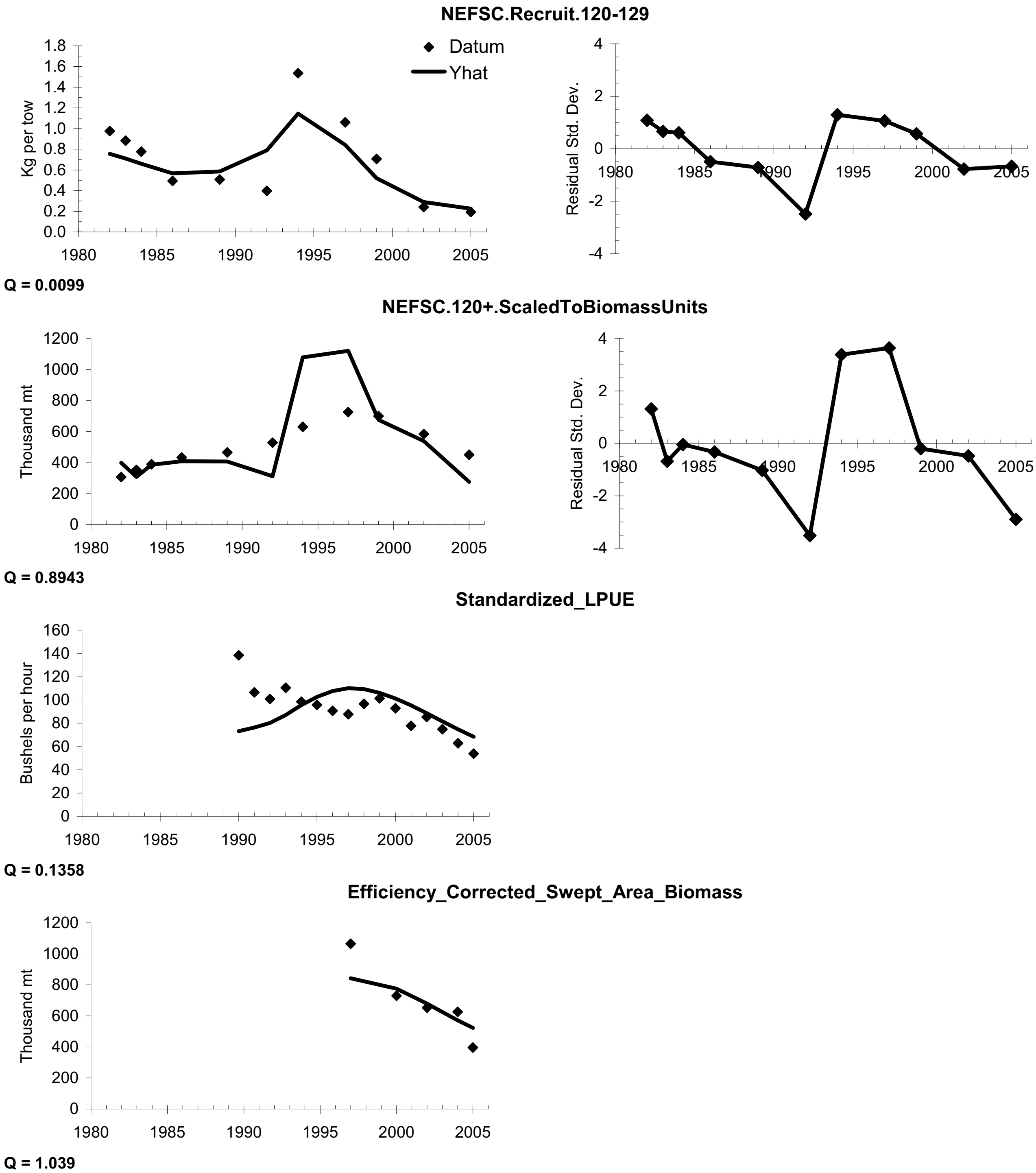

Figure C46. Model diagnostics for the KLAMZ model surfclam in NJ. Trends in nominal LPUE and efficiency corrected swept area biomass are shown with predicted trends from the model for comparison, but trends in these indices did not affect model estimates. Survey scaling parameter (*Q*) estimates are shown below plots for each set of data.

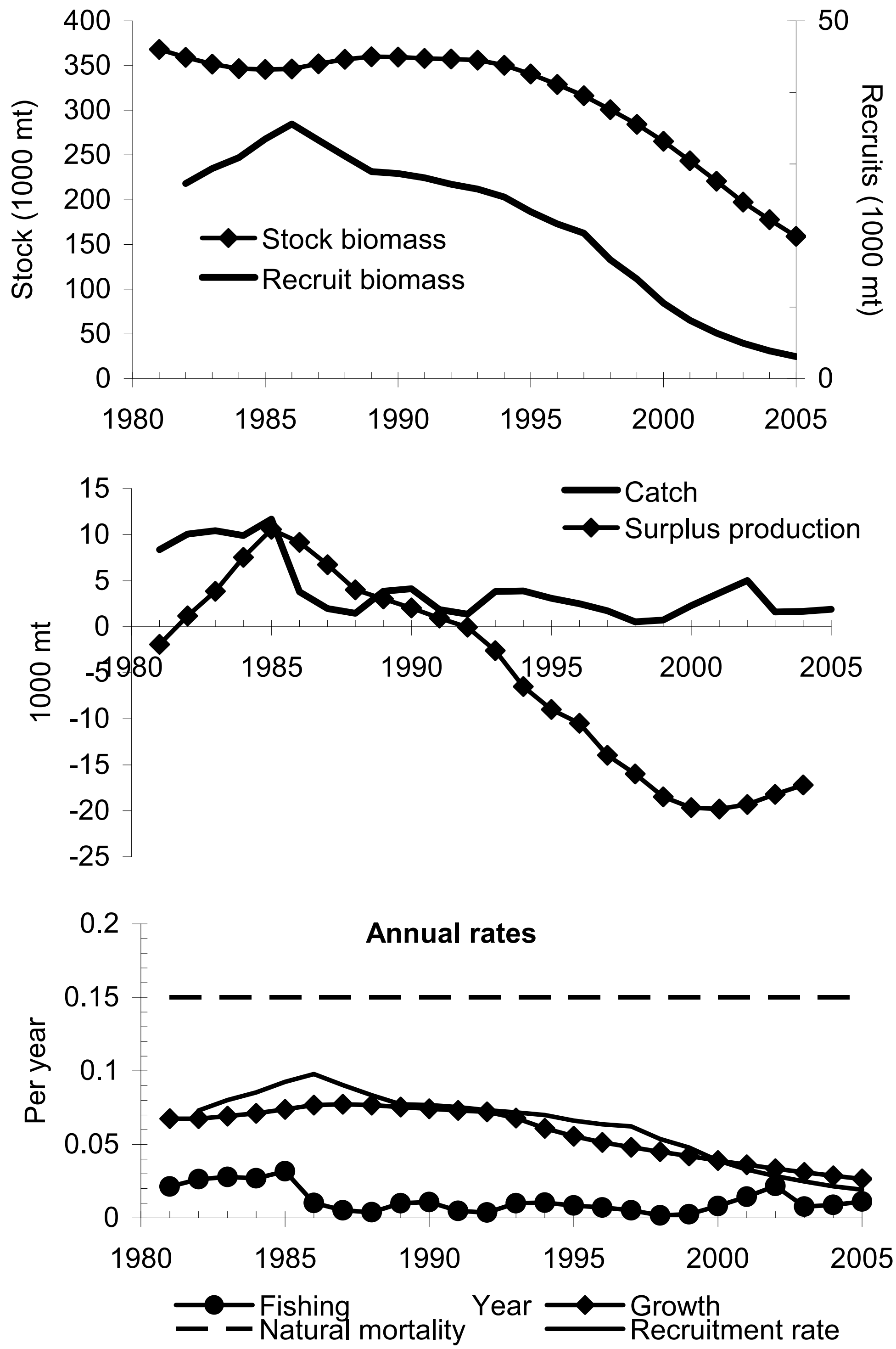

Figure C47. Population dynamics estimates from the KLAMZ model for surfclam in DMV region.

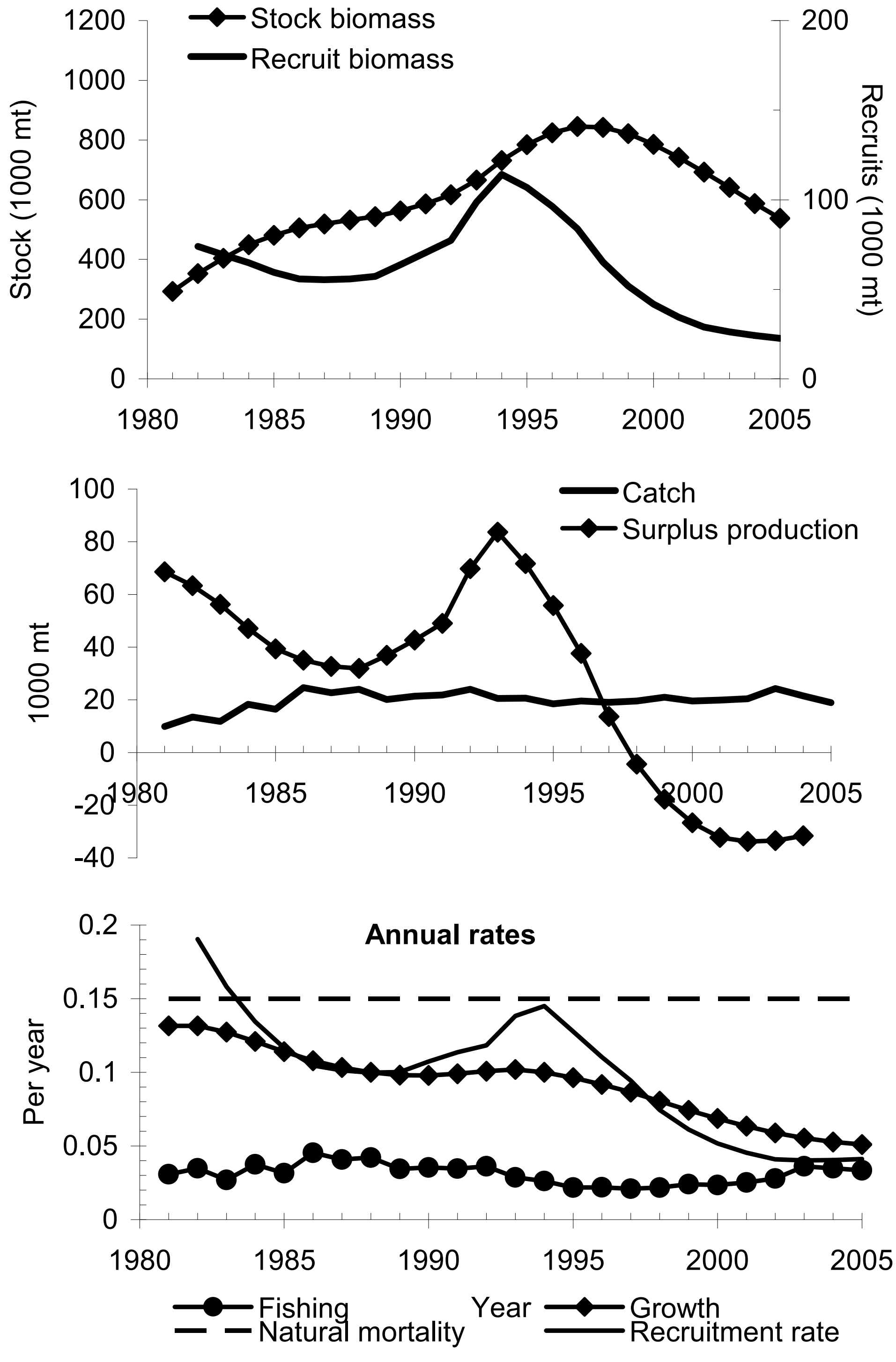

Figure C48. Population dynamics estimates from the KLAMZ model for surfclam in NJ region.

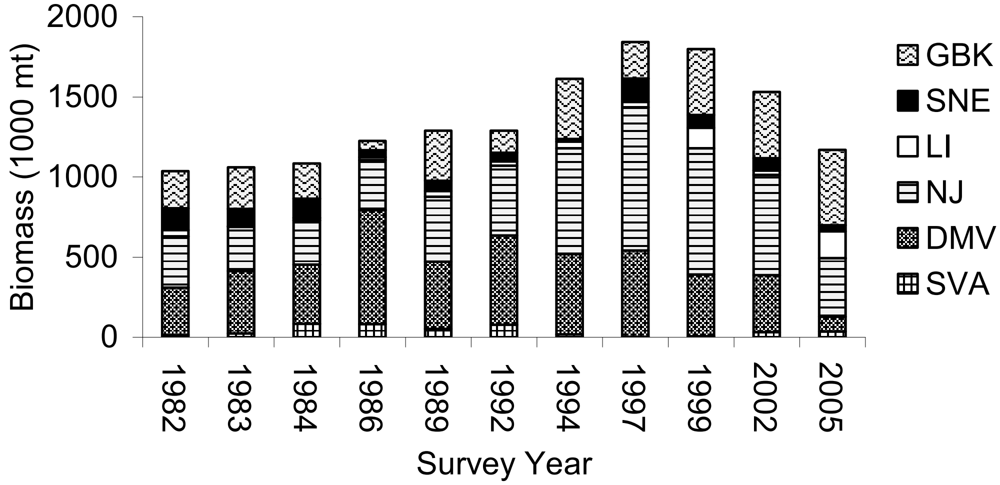

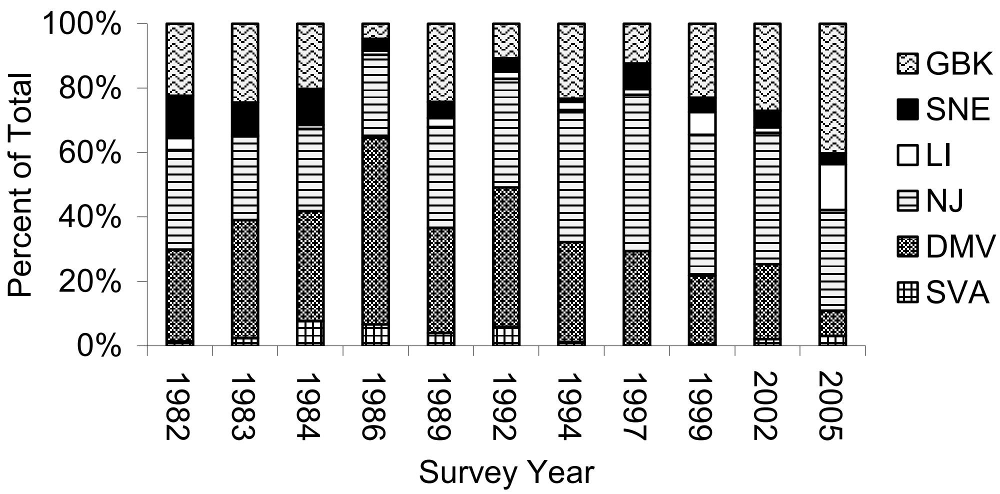

Figure C49. Surfclam biomass for the whole stock prorated into regional components based on rescaled regional survey trend data.

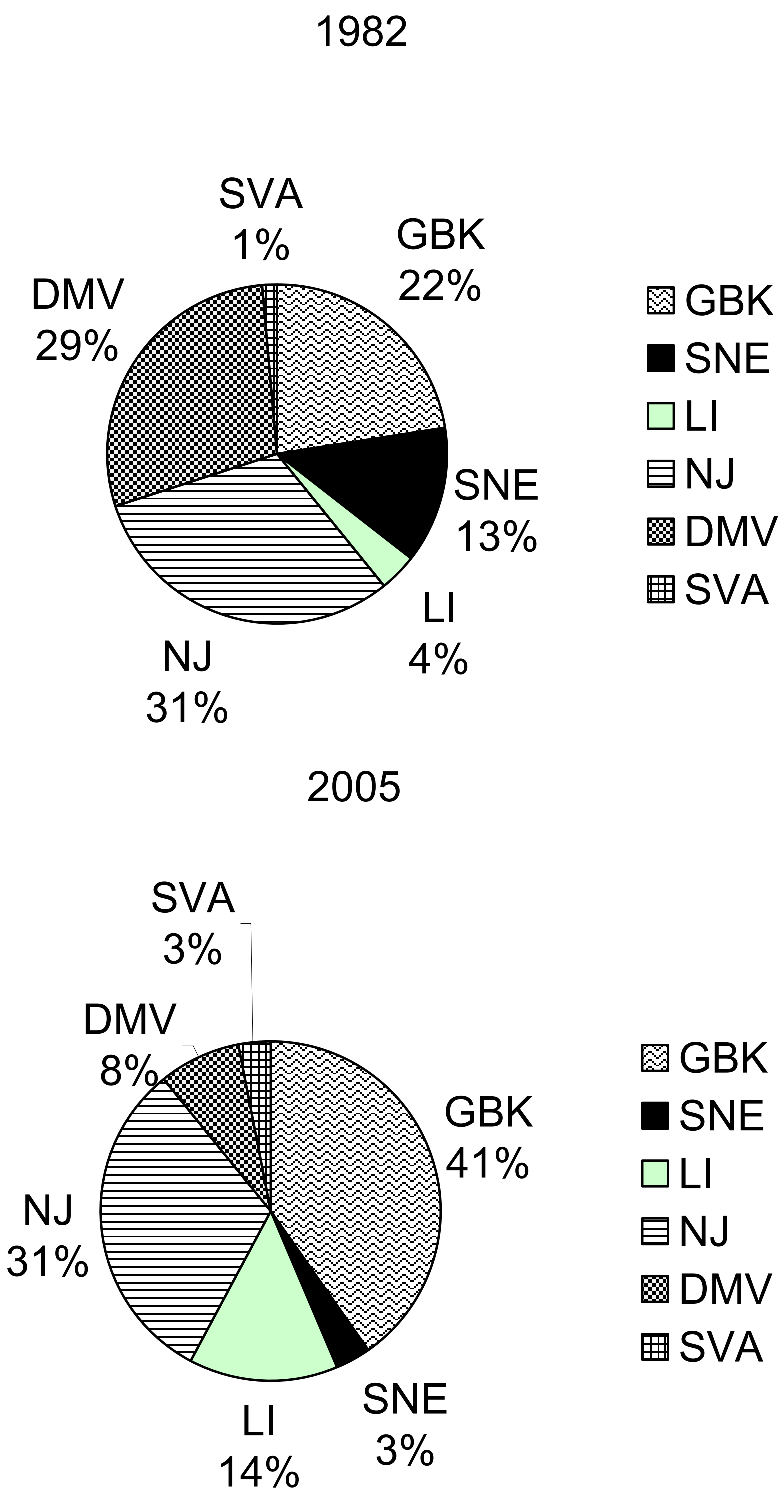

Figure C50. Proportions of total surfclam biomass by region during 1982 and 2005.

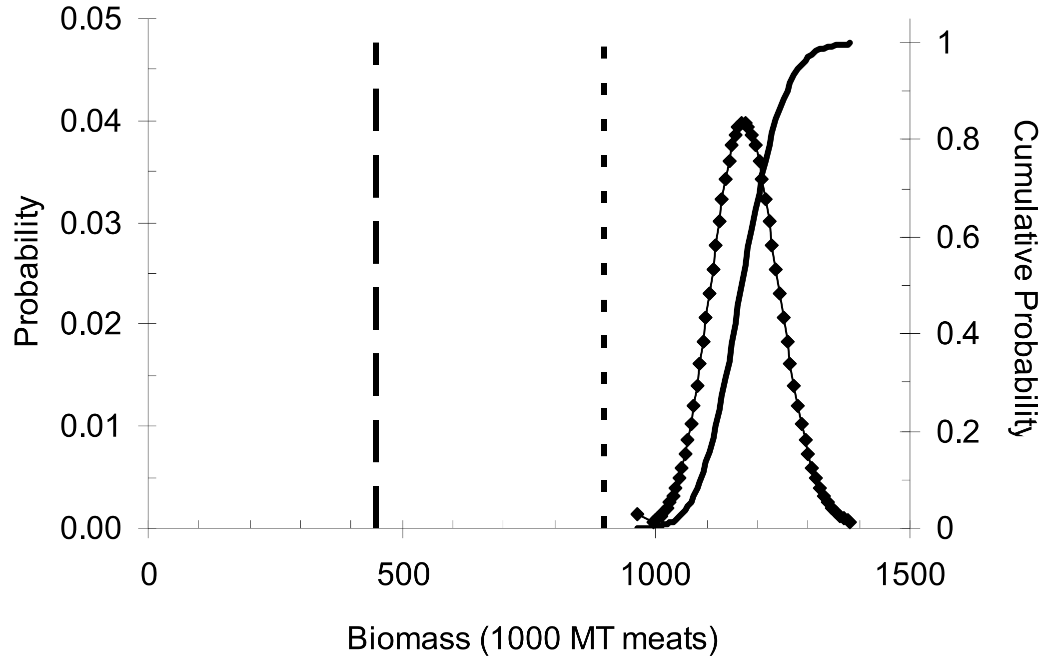

Figure C51. Fishable surfclam biomass during 2005 with probability distributions to characterize uncertainty. The long dash vertical line on the left is the biomass threshold. The short dash vertical line on the right is the biomass target.

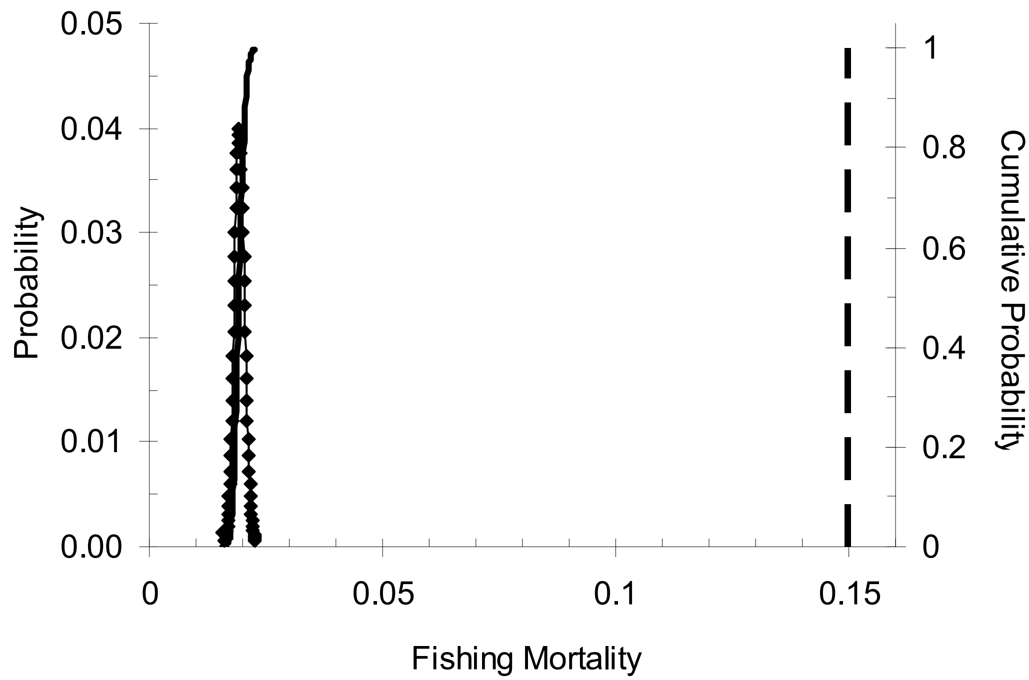

Figure C52. Fishing mortality for surfclam during 2005 with probability distributions to characterize uncertainty. The dash vertical line on the right is the fishing mortality threshold reference point.

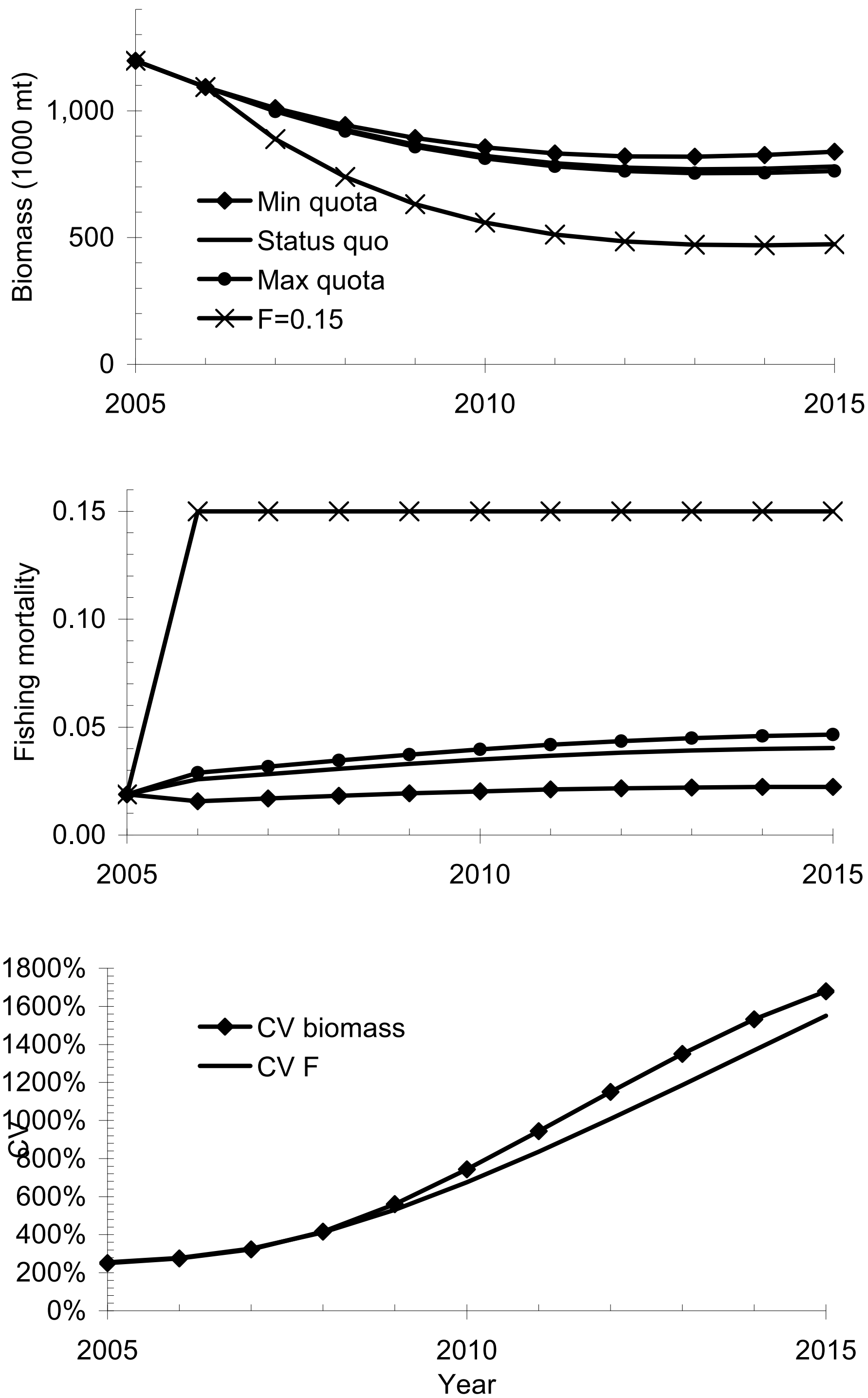

Figure C53. Average biomass and fishing mortality during 2005-2015 based on stochastic projection analysis under four assumed scenarios for constant landings of constant fishing mortality. CVs are for the variability between simulation runs in the same scenario.